



*Citation for published version:*

Arnott, R, Cherif, M, Bryant, L & Wain, D 2021, 'Artificially generated turbulence: A review of phycological nanocosm, microcosm, and mesocosm experiments', *Hydrobiologia*, vol. 848, pp. 961-991.  
<https://doi.org/10.1007/s10750-020-04487-5>

*DOI:*

[10.1007/s10750-020-04487-5](https://doi.org/10.1007/s10750-020-04487-5)

*Publication date:*

2021

*Document Version*

Peer reviewed version

[Link to publication](#)

## University of Bath

### Alternative formats

If you require this document in an alternative format, please contact:  
[openaccess@bath.ac.uk](mailto:openaccess@bath.ac.uk)

#### General rights

Copyright and moral rights for the publications made accessible in the public portal are retained by the authors and/or other copyright owners and it is a condition of accessing publications that users recognise and abide by the legal requirements associated with these rights.

#### Take down policy

If you believe that this document breaches copyright please contact us providing details, and we will remove access to the work immediately and investigate your claim.

1 **Artificially generated turbulence: A review of phycological nanocosm, microcosm, and**  
2 **mesocosm experiments**

3  
4 **Russell N. Arnott<sup>1</sup>, Mehdi Cherif<sup>2</sup>, Lee D. Bryant<sup>1</sup>, Danielle J. Wain<sup>1,a,\*</sup>**

5  
6 *<sup>1</sup>Department of Architecture and Civil Engineering, University of Bath, UK; <sup>2</sup>Department of*  
7 *Ecology and Environmental Sciences, Umea University, Sweden*

8  
9 \*Corresponding author: [danielle.wain@7lakesalliance.org](mailto:danielle.wain@7lakesalliance.org)

10 *<sup>a</sup>Current affiliation: 7 Lakes Alliance, Belgrade Lakes, ME, USA*

11  
12 **Abstract**

13  
14 Building on a summary of how turbulence influences biological systems, we reviewed key  
15 phytoplankton-turbulence laboratory experiments (after Peters and Redondo (1997) and  
16 Peters and Marrasé (2000)) to provide a current overview of artificial-turbulence generation  
17 methods and quantification techniques. This review found that most phytoplankton studies  
18 using artificial turbulence feature some form of quantification of turbulence; it is  
19 recommended to use turbulent dissipation rates ( $\epsilon$ ) for consistency with physical  
20 oceanographic and limnological observations. Grid-generated turbulence is the dominant  
21 method used to generate artificial turbulence with most experiments providing quantified  $\epsilon$   
22 values. Couette cylinders are also commonly used due to the ease of quantification, albeit as  
23 shear rates not  $\epsilon$ . Dinoflagellates were the primary phytoplanktonic group studied due to their  
24 propensity for forming harmful algal blooms (HAB) as well as their apparent sensitivity to  
25 turbulence. This study found that a majority of experimental set-ups are made from acrylate

26 plastics that could emit toxins as these materials degrade under UV light. Furthermore, most  
27 cosm systems studied were not sufficiently large to accommodate the full range of turbulent  
28 length scales, omitting larger vertical overturns. Recognising that phytoplankton-turbulence  
29 interactions are extremely complex, the continued promotion of more interdisciplinary  
30 studies is recommended.

31

32 **Keywords:** phytoplankton, interactions, harmful algal blooms, dinoflagellates

33

#### 34 **DECLARATIONS**

35 **Funding:** Funding for this work was provided by a UK Royal Society International  
36 Exchange Grant IES\R3\170070 awarded to D. Wain and M. Cherif. We also acknowledge  
37 the financial support of the Knut and Alice Wallenberg Foundation (d.nr. 2016.0083).

38

39 **Conflicts of Interest:** None

40

41 **Data Availability:** Not applicable

42

43 **Code Availability:** Not applicable

44

45

46

## 47 INTRODUCTION

48 Turbulence is a key physical characteristic of aquatic systems that has profound impacts  
49 on phytoplankton population dynamics. Many early studies of these complex biological-  
50 turbulence interactions (Figure 1) focussed upon the role of turbulence in homogenously  
51 redistributing phytoplankton species throughout the water column. Stably stratified water  
52 columns typically promote positively buoyant species, allowing them to access increased  
53 light levels and, in nearshore waters, nutrients trapped above the pycnocline associated with  
54 catchment runoff. This scenario is vastly generalised and broadly characterised; additional  
55 studies into the various biological-turbulence interactions have yielded a variety of complex  
56 feedback mechanisms (Figure 1).

57 To understand this array of interconnected feedback mechanisms and accurately predict  
58 how phytoplankton behave in a given environment, researchers frequently adopt one of two  
59 approaches. The first is to model a general phytoplankton population using either a single,  
60 idealised species (Ross and Sharples, 2007; Ross and Sharples, 2008) or a combination of  
61 idealised species, e.g., positively buoyant dinoflagellates against negatively buoyant diatoms  
62 (Huisman et al., 1999). The second approach is to artificially produce turbulence in a  
63 mesocosm facility (hereafter referred to as a cosm to include facilities across an array of  
64 sizes) and expose either a monoculture, a mixture of species, or a natural population to  
65 varying levels of turbulence (Peters and Redondo, 1997). It is the latter that this review  
66 focuses upon.

67 This review begins with an overview of biological-turbulence interactions, drawing upon  
68 key studies to highlight the complex relationship between phytoplankton and turbulence. Best  
69 practice is then discussed with regards to the experimental design of phytoplankton cosm  
70 studies. Building upon this, the main methods of artificial turbulence generation (grids,  
71 shaker tables, aeration and Couette cylinders are discussed and reviewed, with less-

72 commonly used methods included in Appendix 1. This review culminates with a discussion  
73 of the different techniques used to quantify turbulence in cosm experiments, with lesser-used  
74 techniques found in Appendix 2.

75 Note that this review is limited to studies involving phytoplankton in controlled  
76 laboratory settings and, to this end, omits observations of natural systems as well as  
77 biological-turbulence interaction studies on higher trophic organisms (e.g., zooplankton and  
78 fish larvae). A total of 102 publications were used to complete this review. For publications  
79 where more than one generation technique was used, these have been counted as separate (a  
80 total of 8). For single experiments that yielded multiple publications (a total of 14), these  
81 have been counted as a single study. A summary table of all publications used for this review  
82 can be found in Appendix 3.

83

#### 84 **Quantifying Turbulence in Aquatic Environments**

85 Most aquatic environments are turbulent flows comprised of eddies of varying size. As  
86 a fluid is perturbed at the macroscale (e.g., by wind), the energy imparted to that fluid  
87 cascades down from larger to increasingly smaller eddies until is it dissipated by the viscosity  
88 of the water. When measuring turbulence, there are a number of different variables that can  
89 be used to quantify the turbulent field. If we consider the rate at which the kinetic energy  
90 dissipates due to viscous forcing (i.e., the rate of turbulence kinetic energy dissipation;  $\epsilon$ ), it is  
91 possible to quantify turbulence.

92 It is also possible to quantify turbulence via velocity shear. As a fluid flows past a  
93 surface, shear is generated as friction between the fluid and the surface causes a boundary  
94 layer. This layer diffuses away from the surface, perpendicular to the direction of the flow. At  
95 certain thresholds, the boundary layer can give way to vortex shedding as the flow switches  
96 from laminar to turbulent. Within the remit of this review, shear is only used to quantify

97 turbulence in studies that make use of Couette cylinders where shear flow is used to generate  
98 turbulence inside the cylinder. For laboratory measurements to be comparable with those in  
99 the field, it is thus recommended that turbulence values are reported as  $\varepsilon$  in units of  $\text{m}^2/\text{s}^3$ ,  
100 which are the more commonly reported field units across disciplines.

101

## 102 **Study Aim**

103 This review builds upon the seminal work of Peters and Redondo (1997) and  
104 incorporates literature from over the subsequent 20-plus years in order to ascertain best  
105 practice when it comes to laboratory-based turbulence-generation studies. There is clearly the  
106 need for greater standardisation across turbulence studies to facilitate easier and more direct  
107 comparisons between studies. Peters and Redondo (1997) originally set out to “*spark more*  
108 *interdisciplinary science*,” aiming to support biologists by introducing them to the world of  
109 turbulence.

110 As well as discussing the various methods of generating turbulence (along with  
111 accompanied mathematical principles), Peters and Redondo (1997) made a key discovery:  $\varepsilon$   
112 generated in laboratory experiments can commonly be up to orders of magnitude higher than  
113 the average level of  $\varepsilon$  typically observed in the oceanic surface-mixed layer ( $\varepsilon = 10^{-5} \text{ m}^2/\text{s}^3$ ).  
114 Many of the “classic” papers on the effects of turbulence on phytoplankton growth (White,  
115 1976; Pollinger and Zemel, 1981; Savidge, 1981) actually made no attempt to quantify the  
116 levels of turbulence to which their phytoplankton populations were exposed. Thankfully, as  
117 this study area developed over time, practitioners retrospectively quantified their  
118 experiments; it is now standard to include estimates of  $\varepsilon$  and/or other turbulence quantities (  
119 Table I).

120 From descriptions of laboratory set-ups, Peters and Marrasé (2000) estimated that the  
121 level of  $\varepsilon$  in some experiments could have been as high as  $0.23 \text{ m}^2/\text{s}^3$ . Results from

122 experiments with exaggerated levels of turbulence may have water-quality applications such  
 123 as artificial mixing in reservoirs and bathing water (Kirke, 2001; Visser et al., 2016).  
 124 However, if the purpose of the experiment is to accurately model a biological-physical  
 125 system that would occur in a natural aquatic system, then it is crucial for the experimental  
 126 set-up to be as representative as possible of the real world. It is highly prudent to correctly  
 127 quantify the level of turbulence generated prior to commencing a study to ensure that  
 128 experimental conditions are representative of the environment being replicated.  
 129

130 *Table 1 - Comparison of the main turbulence-generation techniques taken from publications*  
 131 *between 1953 to 2020 inclusive (n=102). As well as the number of publications associated*  
 132 *with each technique, we also see the proportion of studies which include turbulence*  
 133 *quantification. See also Figure 6 for a chronology of publications for different turbulence*  
 134 *generation methods.*

<b>Turbulence generation method</b>	<b>Quantified</b>	<b>Quantified Elsewhere</b>	<b>Unquantified</b>	<b>Total Studies</b>
Aeration	1	3	7	11
Couette	15	3	0	18
Grid	29	2	1	32
Shaker	6	9	4	19
Other	14	1	6	21

135

### 136 **Biological-Turbulence Interactions**

137 Turbulence can have a profound influence on individual cells, specific species, and  
 138 community composition in many ways. Most simply, high levels of turbulence can cause  
 139 mechanical destruction by detaching flagella (Pollinger and Zemel, 1981), directly  
 140 impacting motility. Turbulence also acts as a mechanism by which to homogenously  
 141 distribute positively buoyant, motile species throughout a water column or to resuspend  
 142 negatively buoyant, non-motile species; this directly impacts cell access to the photic layer  
 143 and/or the light climate to which a cell is exposed (Kjørboe, 1993; Visser et al., 2016). Thus,  
 144 the turbulent regime of a water body can have a profound impact on the phytoplankton

145 community composition with corresponding effects further along the food web. To this end,  
146 turbulence has been seen to increase both predator-prey encounter rates (Rothschild and  
147 Osborn, 1988) and contact rates between parasites and phytoplankton cell hosts (Llaveria et  
148 al., 2010).

149 At the cell level, turbulence can impact cell growth via altering rates of nutrient uptake  
150 and exposure to light. Phytoplankton cells uptake nutrients from the surrounding water via  
151 diffusion; reduced flow at the cell surface causes the water surrounding the cell (i.e., the  
152 concentration boundary layer) to become nutrient depleted (Prairie et al., 2012) and replete  
153 with waste (Lazier and Mann, 1989; Kiørboe, 1993). Turbulent flows are seen to increase the  
154 laminar shear across the cell surface, eroding the concentration boundary layer and causing a  
155 corresponding increase in nutrient flux to the cell (Lazier and Mann, 1989; Kiørboe, 1993;  
156 Arin et al., 2002; Peters et al., 2006). Conversely, turbulence can also reduce the rate of cell  
157 division (Sullivan et al., 2003) with prolonged exposure to high turbulence intensities  
158 resulting in increased cell mortality (White, 1976; Pollinger and Zemel, 1981). Even short-  
159 duration, high-intensity turbulence applied at a specific time in the cell cycle can inhibit cell  
160 division (Pollinger and Zemel, 1981). Turbulence can also induce the “flashing light effect”  
161 (a.k.a., the light–dark cycle, intermittent illumination, light intensity fluctuation and/or  
162 dynamic light condition;(Sato et al., 2010)) in cells. This phenomenon has been observed to  
163 increase the photosynthetic efficiency in cultured species exposed to intermittent light  
164 fluctuations (Laws et al., 1983; Grobbelaar, 1989) via a reduction in photoinhibition (Nedbal  
165 et al., 1996) thought to be linked to the light fluctuations that a cell would be exposed to  
166 within a turbulent environment.

167 Turbulence also can cause changes in cell morphology. For example, the dinoflagellate  
168 *Ceratocorys horrida* Stein experienced a reduction in cell size and spine length in response to  
169 high turbulent intensities, an adaptation postulated to allow cells to sink below the more



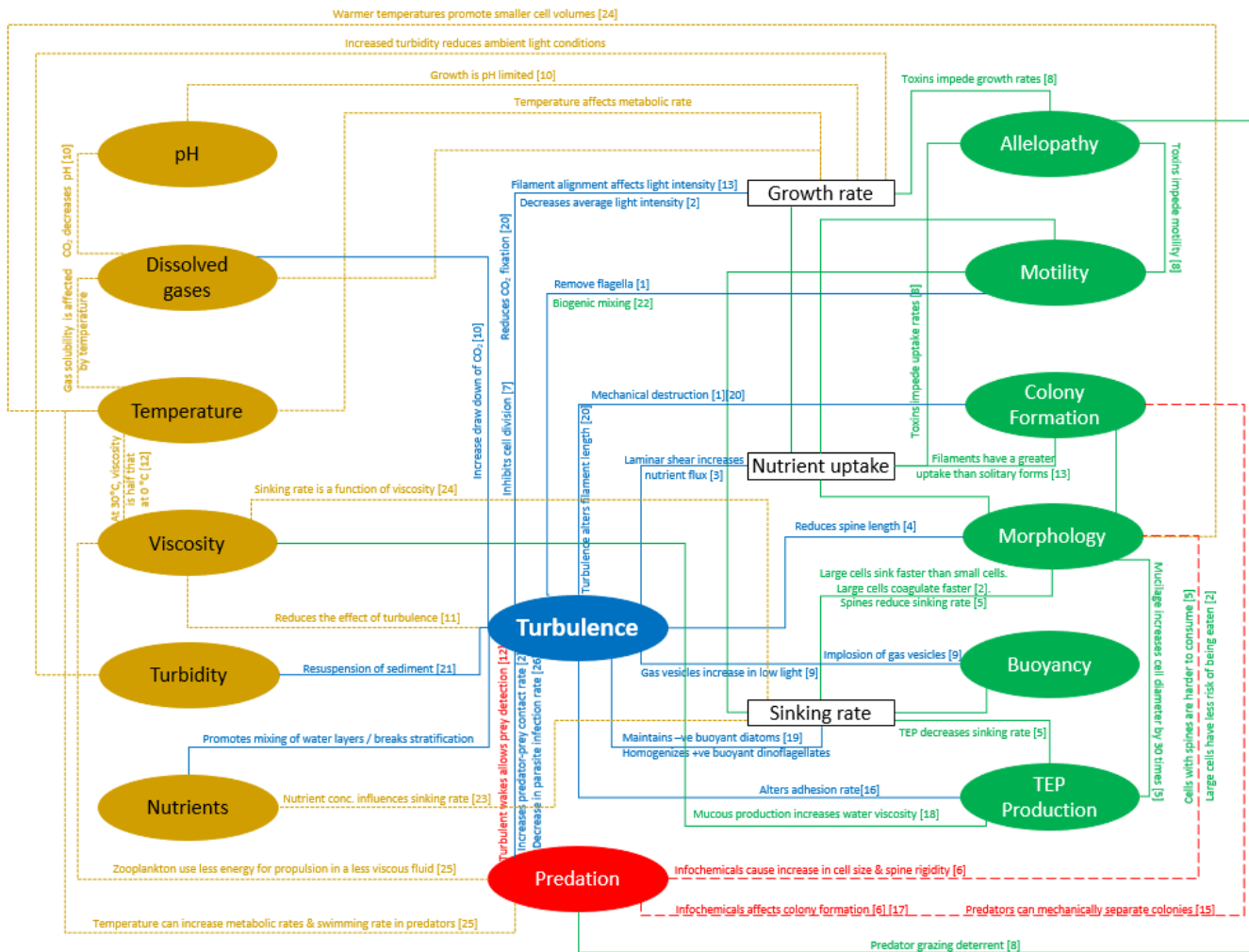
170 turbulent conditions and reduce risk of mechanical damage (Zirbel et al., 2000). Cell  
171 morphology is also linked to light climate with elongated particles becoming aligned in the  
172 direction of flow, thereby increasing the backscatter of light in the water column (Guasto et  
173 al., 2012). Morphology is also linked to nutrient uptake, the rate of which preferentially  
174 increasing in larger cells when compared to smaller cells in turbulent conditions (Guasto et  
175 al., 2012).

176 Further studies linking turbulence to morphology and surface-area-to-volume (SAV)  
177 ratios across different species suggested these parameters to be crucial in determining nutrient  
178 uptake (Fraisse et al., 2015). Growth rate of large species was often exceeded by that of  
179 smaller species in nutrient-limited conditions (Cózar and Echevarría, 2005) whereas shape  
180 dictated how a species behaved hydrodynamically while in turbulent flows and whilst sinking  
181 (Padisák et al., 2003). Clearly, shape and SAV ratios are interlinked; elongated cells were  
182 seen to outcompete spherical cells with regards to nutrient acquisition (Pahlow et al., 1997).

183 Morphology also plays a key role in how colonial, chain-forming filamentous species  
184 interact with turbulent fields; for example, longer filaments sink faster in calm conditions, but  
185 under turbulent conditions a filament can grow to greater sizes as a result of turbulence-  
186 induced increases in light access (Fraisse et al., 2015). Chain-forming, postulated to be a  
187 means for avoiding grazing (Kjørboe, 1993), also provides a mechanism by which to increase  
188 form drag and thereby reduce sedimentation (Padisák et al., 2003). Turbulence has been  
189 observed to separate large colonies, thereby separating filament chains into smaller sections  
190 (Pahlow et al., 1997) which are able to sink and access additional nutrients at depth (Padisák  
191 et al., 2003). The ability of a colony to deform in different flow environments is thought to  
192 give colonial species a competitive advantage in a wider range of turbulent regimes (Guasto  
193 et al., 2012). Turbulence-enhanced nutrient uptake is also seen to preferentially affect  
194 colonies when compared to singular cells (Guasto et al., 2012). Chain-forming species exhibit

195 a range of lengths, orientations and flexibilities, all of which affect their hydrodynamic  
196 properties. Compared to flexible chains, increasingly stiffer chains not only exhibit higher  
197 rates of nutrient consumption but also experience larger nutrient fluxes (Musielak et al.,  
198 2009). With focus on phytoplankton as a carbon pump, colonial diatoms are known to be  
199 prolific fixers of carbon dioxide (CO<sub>2</sub>) where under turbulent conditions, they export carbon  
200 from the upper ocean to depths by forming fast-sinking aggregates. To this end, rates of  
201 turbulence-enhanced carbon uptake have been observed to be higher in chain-forming species  
202 than in individual cells (Bergkvist et al., 2018).

203         The traditional view of phytoplankton behaving as benign passengers at the whims of  
204 forces within the water column holds for macroscale flows; however, the various experiments  
205 described within this review act to showcase a dynamic group of organisms capable of  
206 complex abilities and feedback mechanisms permitting them to gain a foothold over  
207 competing species by altering their properties to suit the conditions of the water column.  
208 Increasingly, researchers are recognising that different phytoplankton have an array of  
209 ecological adaptations that allow them to prosper within an array of various turbulent  
210 environments (Margalef, 1997; Fraisse et al., 2015). With emphasis placed on the effect of  
211 turbulence, Figure 1 allows us to appreciate the complexity of turbulence-plankton  
212 interactions. Further weight is added herein to recommendations found in key papers  
213 (Margalef, 1997; Peters and Redondo, 1997) which characterise turbulence within a water  
214 column to be as significant a biological determinant as temperature or salinity, thereby  
215 emphasising the importance of measuring shifts in phytoplankton communities and  
216 turbulence concurrently.



- [1] Pahlow et al. (1997)
- [2] Kjørboe (1993)
- [3] Lazier and Mann (1989)
- [4] Zirbel et al. (2000)
- [5] Padisák et al. (2003)
- [6] Lürling (1998)
- [7] Pollinger and Zemel (1981)
- [8] Schwartz et al. (2016)
- [9] Walsby (1971)
- [10] Havskum and Hansen (2006)
- [11] Hellung-Larsen and Lyhne (1992)
- [12] Margalef (1997)
- [13] Guasto et al. (2012)
- [14] Leterme et al. (2008)
- [15] Dawidowicz (1990)
- [16] Beauvais et al. (2006)
- [17] Long et al. (2007)
- [18] Smayda and Reynolds (2001)
- [19] Huisman et al. (1999)
- [20] Moisander et al. (2002)
- [21] Visser et al. (2016)
- [22] Katija (2012)
- [23] Bienfang et al. (1982)
- [24] Naselli-Flores et al. (2020)
- [25] Simoncelli et al. (2019)
- [26] Llaveria et al. (2010)

Figure 1 - Flow diagram summarising various links and feedbacks of phytoplankton-turbulence interactions. Green = biological characteristics; white = rates; blue = turbulence processes; red = predation; gold = water properties. Associated coloured text denotes the forcing factor for that link. Where appropriate, links are qualified with numbered references. Dashed lines are included to assist colour-blind readers in distinguishing problematic colours.

## 217 **EXPERIMENTAL DESIGN**

218

### 219 **Facility Considerations**

220 Before evaluating different methods of turbulence generation, the experimental  
221 vessel(s) itself should be considered as something as simple as the shape, scale and material  
222 can considerably influence the experiment if not properly accounted for. As such, the  
223 following section discusses the potential implications of tank volume, tank shape, the material  
224 the tank is constructed from and how the tank is filled.

225

#### 226 *Volume of Tank*

227 Crossland and La Point (1992) posed the question: “*How big does a mesocosm have to be to*  
228 *provide a realistic simulation of the natural environment?*” The answer is very dependent on  
229 the scale and scope of study taking place. Throughout the literature, however, the terms  
230 nanocosm, microcosm and mesocosm are frequently used interchangeably. Whether a cosm is  
231 classed as nano-, micro-, or meso- is open to interpretation with some using volume as the  
232 distinguishing feature (Waller and Allen, 2008; Alexander et al., 2016) while others use  
233 diameter or length (Kangas and Adey, 2008). In summary, Solomon and Hanson (2014)  
234 provided the best characterisation of the different cosms (Table 2). Traditionally, researchers  
235 used small (< 1L) nanocosms described as “simplified, physical models of an ecosystem that  
236 enable controlled experiments to be conducted in the laboratory or in situ” (Matheson, 2008).  
237 Increasing in size leads sequentially to microcosm and mesocosm systems, generally  
238 described to be “bounded and partially enclosed outdoor experimental setups falling between  
239 laboratory microcosms and the large, complex real world macrocosms” (Odum, 1984). These  
240 facilities may be housed inside or outdoors (i.e., on land or in water) depending on the nature  
241 of the setup. For outside enclosures suspended within an aquatic environment, Solomon and

242 *Table 2 - Characterisation of different cosms. After Solomon and Hanson (2014).*

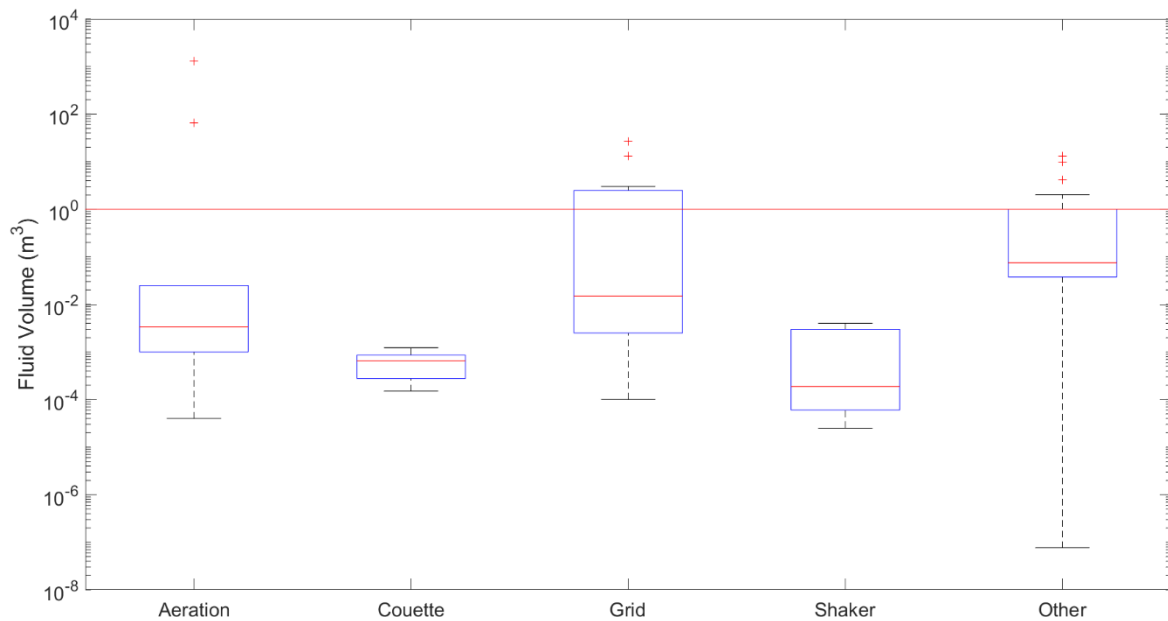
	<b>Nanocosm</b>	<b>Microcosm</b>	<b>Mesocosm</b>
<b>Volume (L)</b>	1 – 100	100 - 15000	>15000
<b>No. of Trophic Levels</b>	2	3+	3+
<b>Optimum study duration</b>	<8 weeks	<1 season	>1 season
<b>Typical Location</b>	Inside	Inside or outside	Outside

243

244 Hanson (2014) suggested the term ‘limnocorral’ to differentiate these from facilities on land  
 245 while Parsons et al. (1978) opted for a controlled ecosystem enclosure.

246 With regards to biological studies, a larger experimental volume supports greater  
 247 biodiversity and allows for a larger number of trophic levels to be observed concurrently  
 248 (Alexander et al., 2016); conversely, smaller microcosms typically exclude higher trophic  
 249 levels due to size constraints (Matheson, 2008). With regards to turbulence, vertical overturns  
 250 are known to exist between  $10^{-3}$  to  $10^1$  m; while smaller cosms represent the smaller end of  
 251 this range, clearly a much larger tank would be required in order to capture the upper range.  
 252 After all, it is not possible to produce a 10 m vertical overturn if the tank itself is shallower  
 253 than 10 m depth. Using cosm volume as an indicator of maximum turbulent overturn size  
 254 within a particular experiment, a majority of studies were found to use fluid volumes smaller  
 255 than  $1 \text{ m}^3$  (Figure 2). As expected, it is larger volume limnocorral studies that make up a bulk  
 256 of the experiments above this  $1 \text{ m}^3$  threshold.

257



258

259 *Figure 2 - Boxplots of approximate fluid volumes involved with different types of turbulence-*  
 260 *generation experiments. Central line in each box is the median; top and bottom of each box*  
 261 *indicate the 25th and 75th percentiles. Whiskers extend to the most extreme data points not*  
 262 *considered outliers, with outliers plotted as plus-signs. Continuous horizontal line indicates a*  
 263 *volume of 1 m<sup>3</sup>, considered to be the minimum volume required to capture realistic turbulence*  
 264 *length scales Note the log scale on the y-axis.*  
 265

## 266 *Shape of Tank*

267 Peters and Redondo (1997) put forth the assumption that biologists tend to use  
 268 cylindrical tanks as, in theory, these display a higher degree of homogeneity. Conversely,  
 269 physical studies are generally undertaken in cuboid tanks as the corners disrupt secondary  
 270 flow effects; at the same time, modelling flow within square-based tanks is considered  
 271 simpler mathematically. However, cuboid tanks are considered less homogenous overall due  
 272 to the presence of corners (Peters and Redondo, 1997) which can cause 1) material to collect,  
 273 2) organisms to grow there and/or 3) changes in the turbulent field. In a comparison between  
 274 turbulence generated in smooth- and baffled-bottom flasks,  $\epsilon$  values were seen to be two  
 275 orders of magnitude higher in the latter (Kaku et al., 2006). The shape of a tank can clearly  
 276 play a significant role in the turbulence regime within.

277 Matheson (2008) acknowledged the importance of SAV ratio in microcosm design;  
278 those with a large SAV ratio can promote edge communities of biofilms or cause other  
279 organisms to congregate to avoid predation. As such, these biological “wall effects” can add  
280 significant bias into an experiment; efforts should hence be made to use facilities with small  
281 SAV ratios. The size and aspect ratios of the test vessel would be expected to affect the  
282 growth rate for many reasons. High-volume growth “ponds” (i.e., vessels with a shallow  
283 depth but increased exposed water surface area) are designed to maintain as much of the  
284 population in the photic layer as possible while also reducing the effects of shadowing. A  
285 larger exposed water surface area would not only increase gas exchange across the boundary  
286 but would also promote a higher evaporation rate.

287

#### 288 *Material of Tank*

289 Vessels may be constructed out of an array of different materials depending on  
290 availability and size requirements. Firstly, it is essential that the material of the tank does not  
291 influence the fluid medium inside the tank. As such, it is not advised to use ferrous materials  
292 to construct mesocosms as not only does this add iron to the fluid medium (which is a  
293 photosynthesis-limiting micronutrient; (Martin and Michael Gordon, 1988) but the tank itself  
294 is also at risk of corrosion, especially if using saline fluid media.

295 Other materials may also cause micronutrients to be leached into the culture medium;  
296 glass has the potential to provide a source of silicon, known to be a limiting nutrient for  
297 diatoms (Kilham, 1971). Hellung-Larsen and Lyhne (1992) studied the effects of vessel  
298 material on the rates of cell division in the protozoan *Tetrahymena* sp. and observed no  
299 significant difference when using glass, siliconized glass and plastic.

300 With an increasing propensity for ecologists and other researchers to experiment with  
301 three-dimensional (3D) printing technology, it has been observed that certain extrusion

302 materials, particularly resins, remain toxic to aquatic organisms for some time. Should a  
303 microcosm tank be 3D-printed in resin, however, exposure to ultraviolet (UV) light can  
304 reduce its toxicity substantially (Behm et al., 2018).

305         Conversely, many cosms are constructed from artificial polymers such as acrylate,  
306 polyvinyl-chloride (PVC) and polycarbonate which all undergo photodegradation reactions  
307 under UV light (Yousif and Haddad, 2013), potentially releasing toxins that could adversely  
308 influence productivity. In a similar vein, the presence of polystyrene nanoplastics were seen  
309 to reduce the chlorophyll content of the diatom *Chaetoceros neogracilis* VanLandingham  
310 with subsequent implications on cellular growth and photosynthetic efficiency (Gonzalez-  
311 Fernandez et al., 2019). As such, it is crucial that the tank material itself is not influencing the  
312 growth rate of the organisms being studied. Some plastics are also permeable to certain gases;  
313 depending on the nature of the study, this should also be considered and may even be  
314 desirable (Matheson, 2008).

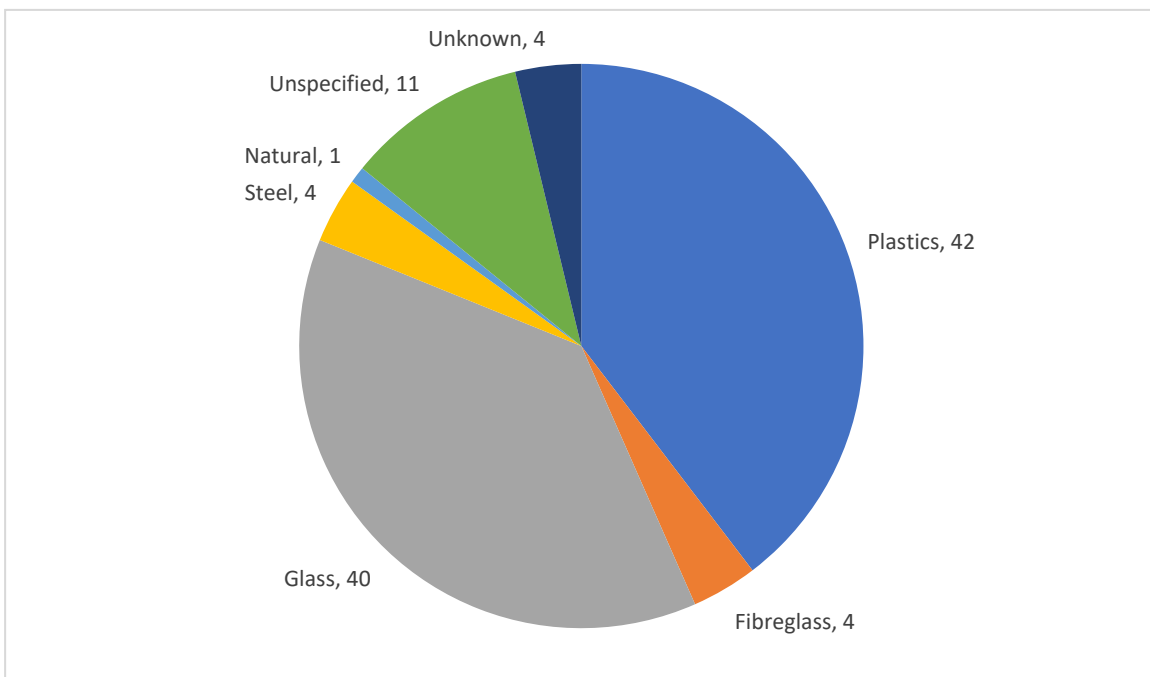
315         As well as releasing chemicals into tank water, certain cosm materials can absorb  
316 chemical species from the water (Kangas and Adey, 2008). Zhou et al. (2016) submerged  
317 Plexiglass tanks in water for 15 days prior to their experiment to allow the tanks to absorb  
318 and/or release any chemicals and equilibrate accordingly. Of the cosms studied, a third was  
319 comprised of plastics that undergo UV degradation (Figure 3). Another third was made of  
320 glass which may be correlated to the high proportion of studies using glass Couette cylinders  
321 and Pyrex vessels on shaker tables.

322         Typically, biologists cultivate cells in transparent vessels to maximise incident light  
323 that allows cells to reproduce further. This eliminates any light gradient within the tank that  
324 would be present in nature. As such, it is advised to use opaque materials when studying the  
325 effects of turbulence; this generates a light-gradient through the tank which can have a  
326 significant impact on results, especially when using phototactic or motile species or those



327 with the ability to regulate their buoyancy. It should also be noted that while surface shading  
328 is a natural phenomenon that regulates phytoplankton growth, light introduced through  
329 transparent walls is susceptible to biofilm growth resulting in decreased light levels over time  
330 (Matheson, 2008). Some practitioners have avoided this effect via a periodic scrubbing of the  
331 tank walls with a brush or similar (Zhou et al., 2016).

332



333

334 *Figure 3 - Materials used in cosm design (based on n=102 studies). Plastics refers to tanks*  
335 *comprised of acylate, polycarbonate, polyethylene and polyvinyl chloride, all of which are*  
336 *known to undergo UV degradation. Glass refers to both standard glass and Pyrex. For cosms*  
337 *comprised of more than one material (n = 2), these materials have been counted separately.*  
338

### 339 *Filling*

340           Phytoplankton-turbulence studies that use smaller nano- and microcosms typically  
341 study the effects of one or two different species at a time based on seeding of the cosms with  
342 laboratory-cultivated cells grown in incubators. However, larger mesocosms and limnocorrals  
343 are typically used to look at natural planktonic communities that may be comprised of  
344 multiple trophic levels and organisms of different sizes. Land-based facilities are typically  
345 filled via pumping offshore waters from a particular depth into the enclosures (Båmstedt and

346 Larsson, 2018). Ideally, sets of cosms will be filled simultaneously or as close timed as  
347 possible to insure homogeneity across all replicate cosms. It is important that the pump filling  
348 system does not inadvertently preclude any larger species nor damage them in their transport  
349 through the pump system (Striebel et al., 2013). Some facilities are able to filter certain size  
350 fractions from the inflow water (Båmstedt and Larsson, 2018), thereby allowing e.g.,  
351 microzooplankton through but omitting mesozooplankton that might graze upon certain size  
352 fractions or cause morphological changes via infochemicals (Long et al., 2007; Figure 1).

353

### 354 **Environmental Variables**

355       Having evaluated potential issues that may arise within different facilities, we next  
356 considered how environmental variables within the cosms may be influenced by particular  
357 experimental setups. Specifically, we looked at the implications of study duration, nature of  
358 the turbulence generated, light climate within the tank and general properties of the water  
359 itself.

360

#### 361 *Duration of study*

362       As suggested by Table 2, the duration of a study is somewhat dictated by the volume  
363 of the tank, with larger facilities being able to accommodate a higher number of trophic levels  
364 (Solomon and Hanson, 2014). It stands to reason that any change in the turbulent regime  
365 within the tank will take time for its effects to cascade through a wider array of trophic  
366 communities. Depending on the rate of cell division across different species (and given  
367 conditions that promote or inhibit growth), it is expected that a phytoplanktonic community  
368 would adjust to a new turbulent regime within a few days. Given a minimum cell division rate  
369 of ~0.5 divisions per day (Banse, 1991), two days should account for cells to replicate at least  
370 once.

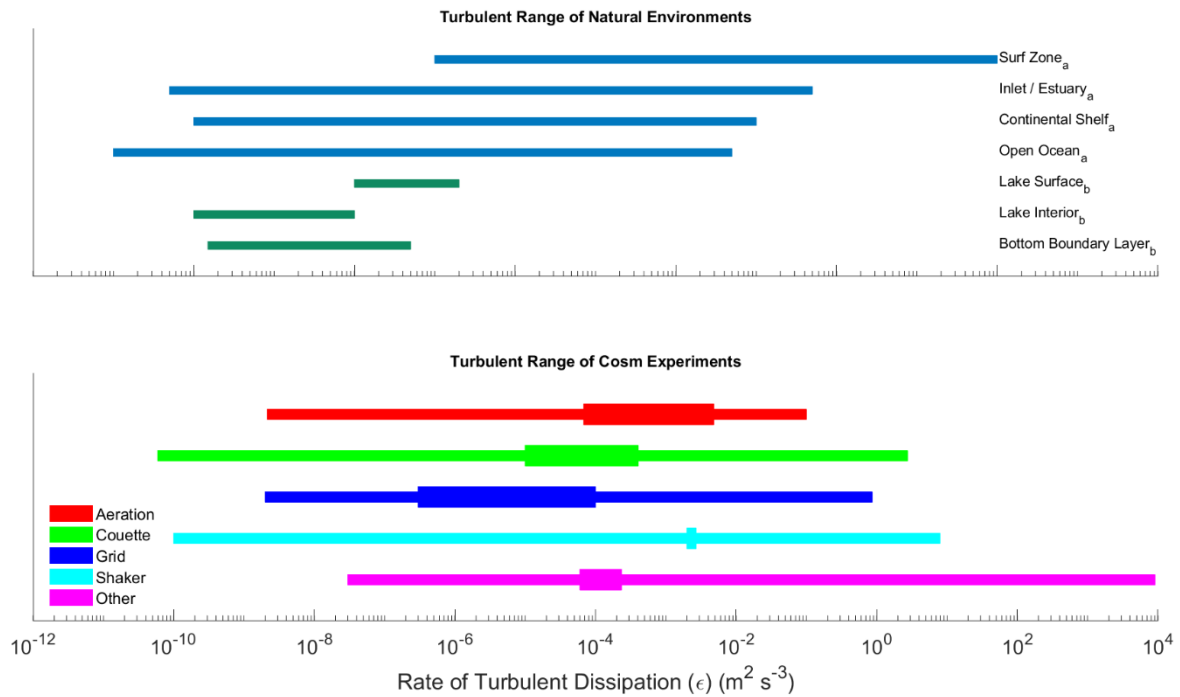
371 It is important to account for the effects of turbulence on growth due to changes in  
372 light regime (Kjørboe, 1993), changes in cell division rate (Pollinger and Zemel, 1981) and  
373 morphological changes to future generations (Zirbel et al., 2000). Once the new turbulent  
374 regime is established and the community adjusts accordingly to the new physical  
375 environment, ecological processes will dominate in regard to inter-species and trophic  
376 interactions.

377

### 378 *Intensity or level of turbulence*

379 If the purpose of conducting laboratory experiments is to ascertain the effect(s) of  
380 turbulence on a planktonic population, then it is crucial for the generated turbulence to  
381 properly represent the real-world, naturally turbulent environment to which organisms would  
382 be exposed. Using large, external limnocorrals may seem to be the easiest way to ensure that  
383 the turbulence within a cosm is as natural as possible; however, it has been observed that  
384 enclosing a portion of a water body within a cosm can significantly reduce the internal mixing  
385 regime when compared to conditions immediately outside the enclosure (Striebel et al., 2013).

386 As well as the tendency to produce excessive and unrealistic levels of turbulence  
387 within a cosm (Peters and Marrasé, 2000), there are a number of reasons to rethink existing  
388 approaches to artificially generated turbulence. It is important to consider how turbulence  
389 manifests itself within aquatic environments where turbulence is generally relatively weak.  
390 Observations suggest that  $\epsilon$  typically exists between  $10^{-10}$  and  $10^{-7}$   $\text{m}^2/\text{s}^3$ , both in central ocean  
391 systems (Fuchs and Gerbi, 2016) and freshwater lakes (Wüest and Lorke, 2003). While wind-  
392 mixed and convectively mixed surface layers seldom exceed  $10^{-5}$   $\text{m}^2/\text{s}^3$  in the open ocean, surf  
393 zone  $\epsilon$  values of up to  $10^{-2}$   $\text{m}^2/\text{s}^3$  have been observed (Fuchs and Gerbi, 2016). Of the  
394 experiments reviewed here, a majority focused on the upper range of  $\epsilon$  found in natural  
395 environments (Figure 4).



396

397 *Figure 4 – Upper: comparison of range of turbulent dissipation rates ( $\epsilon$ ) found in marine and*  
 398 *lacustrine environments taken from Fuchs and Gerbi (2016)(<sub>a</sub>) and Wüest and Lorke*  
 399 *(2003)(<sub>b</sub>) respectively. Lower:  $\epsilon$  produced from turbulence-generation studies evaluated for*  
 400 *this review ( $n = 102$ ). Horizontal lines span total ranges (thin lines) with the lower and upper*  
 401 *log-median  $\epsilon$  limits (thick lines) for each generation method.*  
 402

403 In addition to being relatively weak, turbulence in natural environments can be highly  
 404 sporadic, both temporally and spatially (Waterhouse et al., 2014). Thus, laboratory  
 405 experiments that constantly force turbulence generation and aim for isotropic conditions  
 406 across relatively small tank volumes are unrepresentative of natural conditions. In particular,  
 407 direct and indirect turbulence avoidance strategies have been observed in planktonic  
 408 organisms at a number of trophic levels (Franks, 2001; Pringle, 2007). Thus, for a cosm to  
 409 properly represent the natural environment, a refuge region of less-turbulent water should be  
 410 incorporated into the experimental design to allow the organisms some respite from intense  
 411 turbulence and to facilitate natural behavior (Franks, 2001). It is thus recommended that  
 412 experimental designs of cosms need to be large enough to include this refuge region. While  
 413 this is thought to be particularly applicable to zooplankton studies, many motile

414 phytoplankton species position themselves within the water column to obtain light and/or  
415 nutrients and would also benefit from tank refuge regions.

416

#### 417 *Light*

418 Many standard biological growth facilities are designed to maximise growth with  
419 regards to the light climate of the vessel. As mentioned previously, it is crucial for incident  
420 light within turbulence-generation tanks to attenuate with depth. The biological-turbulence  
421 interactions that underpin the critical depth hypothesis (Sverdrup, 1953) would be invalidated  
422 if light-levels did not attenuate with depth.

423 With regards to the light spectrum that organisms are exposed to, it is best to use  
424 direct sunlight to capture all spectrographic components of the sun at surface level. While this  
425 will be the natural default in outdoor facilities and limnocorrals, indoor facilities traditionally  
426 have relied on filament lamps that had a tendency to over-represent light within the infrared  
427 parts of the spectrum, causing heating to the cosm surface and various thermal lid effects  
428 (Båmstedt and Larsson, 2018). Conversely, filament lamps under-represent the UV  
429 component of sunlight and, while UV light is attenuated quickly in the water column, it can  
430 still have an influence on cosm ecology. For example, waters with high levels of coloured  
431 dissolved organic matter (CDOM) have been shown to increase the attenuation of visible  
432 light, thereby reducing the depth of the upper photic layer (Reynolds, 2009). CDOM  
433 preferentially absorbs visible light towards the blue end of the spectrum as well as UV. The  
434 UV light interacts with an array of complex compounds found in CDOM, causing them to  
435 decompose into smaller compounds which can more easily interact with other biochemical  
436 processes. Thus, the presence of CDOM in the water column can have a profound impact on  
437 primary productivity with depth (Coble, 2007). Paczkowska et al. (2017) showed the explicit  
438 link between CDOM and the phytoplanktonic community; as CDOM degrades in the

439 environment, it provides an important nutrient supply for heterotrophic bacteria which are a  
440 potential food source for any mixotrophic species. Furthermore, under the restricted light  
441 conditions associated with CDOM, phytoplankton respond by increasing the cellular  
442 concentration of the photosynthetic pigments, including chlorophyll-*a*. These restricted light  
443 conditions can also promote a shift towards species with smaller cell sizes (Paczkowska et al.,  
444 2017).

445         With the advent of halogen and LED lights, it is now easier to reproduce the surface  
446 sunlight spectrum within indoor cosms, accounting for UV, visible and infrared components  
447 accordingly. Care should still be taken to measure the photoactive radiation (PAR) within the  
448 cosm to ensure it is attenuating sufficiently with depth and is not too bright to cause photo-  
449 inhibition of cells. As for the duration of light exposure, it is recommended that the day-night  
450 cycle match that of the natural levels the organisms would experience. While a simple binary  
451 on-off timer may be used to achieve this, it is better to include faders in the cosm facility  
452 design to gradually increase or decrease light levels over the course of the day as they would  
453 occur in nature.

454         Additionally, the potential for the turbulence-generation apparatus in a cosm to shade  
455 the water below should be considered. Placing grids, paddles, impellers and similar structures  
456 into a tank can decrease the amount of surficial light that reaches the bottom of cosm. This  
457 was considered to be an issue in a study by Rijkeboer et al. (1990), who promptly replaced a  
458 steel paddle with a transparent Perspex one to minimise this effect.

459

#### 460 *Temperature and salinity*

461         As with light levels, it is also prudent to expose test organisms to temperatures and  
462 salinities that they would ordinarily be subject to in natural aquatic environments. While  
463 temperature has the ability to directly alter photosynthetic and respiration rates in

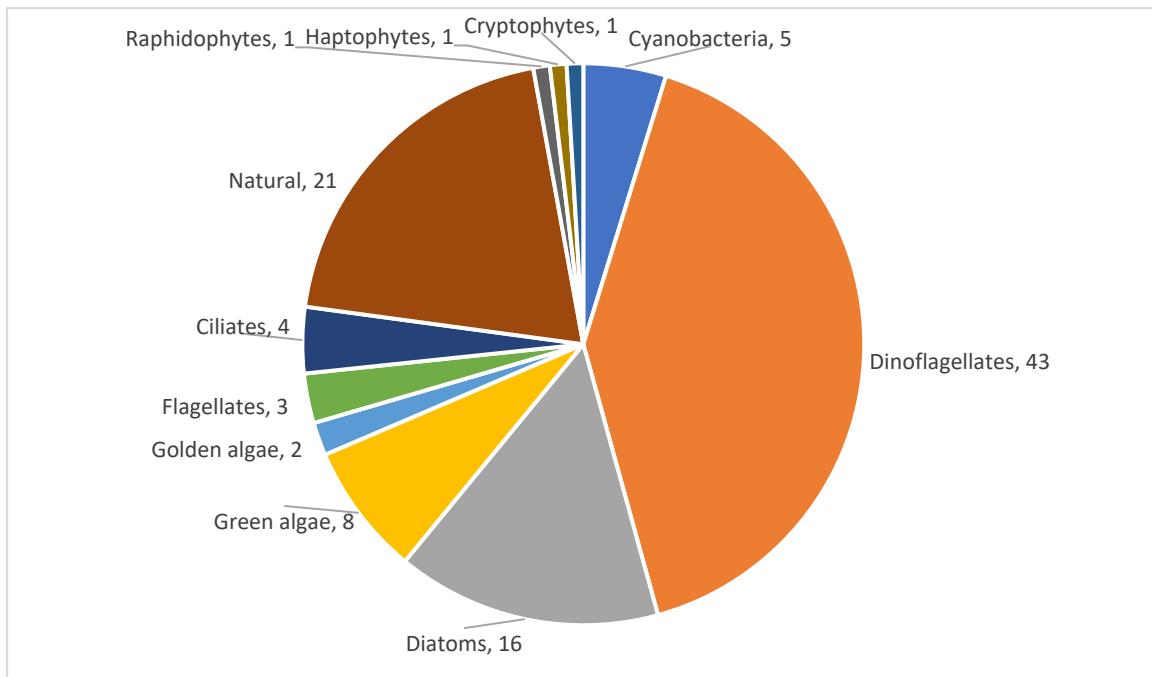
464 phytoplankton (Staeher and Sand-Jensen, 2006), there are also indirect temperature effects  
465 including variations in the solubility of gases. Both temperature and salinity have an influence  
466 on water viscosity which could affect microscale turbulence dynamics. In addition,  
467 temperature has been found to be inversely related to cell volume (Naselli-Flores et al., 2020),  
468 resulting in additional hydrodynamic variations that need to be considered.

469

## 470 **Biological considerations**

471 While smaller nano- and microcosm experiments lend themselves well to studying the  
472 effect of turbulence on a single species, larger mesocosms can be used to investigate  
473 interactions between two (or more) species (Havskum, 2003; Stoecker et al., 2006; Pannard et  
474 al., 2007; Fraisse et al., 2015; Martínez et al., 2017). Due to their apparent sensitivity to  
475 turbulence as well as their propensity to form harmful algal blooms, a majority of studies have  
476 understandably focussed on the dinoflagellate group (Figure 5). Furthermore, this group  
477 includes species with bioluminescent abilities; the light intensity emitted can be used as a  
478 proxy for turbulent shear, thereby facilitating the quantification of shear in cosm experiments  
479 (Stokes et al., 2004).

480 If using a natural planktonic population, it is possible to omit micro-zooplankton by  
481 filtering the water used prior to filling the cosms (Båmstedt and Larsson, 2018). While this is  
482 not suitable for predator-prey interaction studies, the removal of grazing should allow the  
483 subtle impacts of turbulence interactions on the phytoplankton community to be more easily  
484 observed. Choosing the correct filter to omit zooplankton grazers but not affect the larger size  
485 fraction of phytoplankton can be difficult due to the overlap in sizes of these groups. It is also  
486 likely that a natural phytoplankton population might contain mixotrophic ciliates and  
487 dinoflagellates that graze on other species.



488

489 *Figure 5 - Proportion of different phytoplanktonic groups used in the evaluated turbulence-*  
 490 *interaction experimental studies. Number of publications featuring that group is included next*  
 491 *to each segment. "Natural" refers to experiments that made use of indigenous populations.*

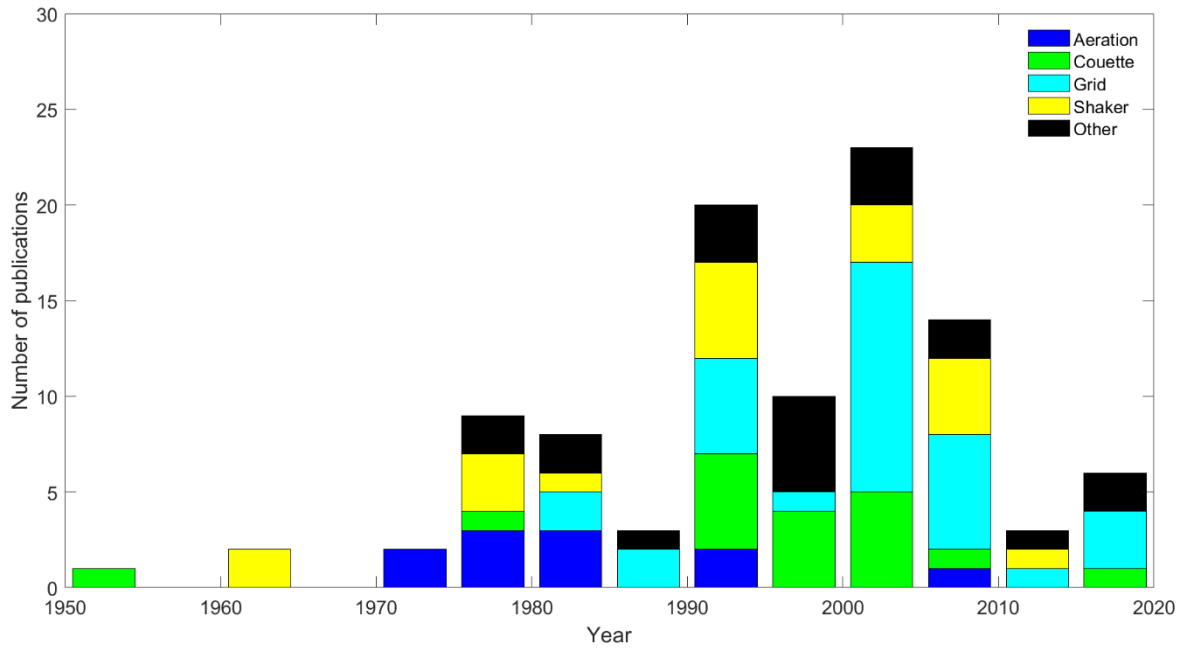
492 **METHODS OF TURBULENCE GENERATION**

493 There are many ways to artificially generate turbulence in a laboratory environment;  
 494 reviews of each of these different techniques and notable case studies for each are provided in  
 495 this section. An analysis of previous methods identified that most studies use just four  
 496 different methods: bubbling aeration, Couette cylinders, oscillating grids and laboratory  
 497 shaker tables.

498 The chronology of publications (Figure 6) mirrors the information displayed in

499 Table 1; clearly grid-generated turbulence is the “industry favourite” with regards to  
 500 phytoplankton-turbulence studies. Despite a boom in studies between 2000 and 2010, the  
 501 recent decade has seen a decline of bio-turbulence publications; the lowest since the pre-  
 502 1970s.





503

504 *Figure 6 – Stacked bar chart of phytoplankton-turbulence publications by year showing the*  
 505 *proportion of different turbulence-generation techniques used.*

506

507 **Oscillating grids**

508 A standard way to generate turbulence within a tank is to use a grid mesh which is  
 509 placed in the tank and connected to a mechanism that allows that grid to move through the  
 510 water. This technique, referred to as “*a favourite in fluid dynamics experiments*” (Guadayol et  
 511 al., 2009b) is often the preferred method of turbulence generation due to its simplicity as well  
 512 as its established use in an extensive number of studies of this nature. Grids are typically of a  
 513 similar width / diameter to the test tank and are a simple way to ensure a consistent turbulent  
 514 field across the width of a tank. Typically, the grids are attached to a motor that allows them  
 515 to oscillate vertically or horizontally at a given frequency and stroke length. A majority of  
 516 these studies quantify  $\varepsilon$  (

517 Table 1; Figure 6) whereas early experiments simply used motor settings or revolutions-  
 518 per-minute (rpm) as a proxy for turbulence intensity.

519 As with the tank material, the grid itself can be made from any material but it is  
520 important that the grid does not corrode or deteriorate with time and remains biologically  
521 inert. For this reason, the use of ferrous metals is discouraged as these materials will not only  
522 degrade in saline water but will also provide a source of iron micro-nutrients. Netlon meshes  
523 are typically used as they come in a variety of mesh-sizes and are hardwearing, easily  
524 available, and corrosion-resistant. It is also possible to coat metal grids in inert substances  
525 such as nylon (Savidge, 1981).

526 In a thorough comparison between turbulence generated by grids to orbital shakers,  
527 Guadayol et al. (2009b) measured turbulence generated in a variety of different sized vessels  
528 ranging from small 0.8 L nanocosms up to 2500 L microcosms. As well as tank size, different  
529 grid configurations were trialled with variations in mesh size, bar width, grid diameter and  
530 cross-sectional shape. Study results show that the turbulence generated using grids was  
531 surprisingly isotropic (especially given the array of tanks size, grid dimensions and oscillation  
532 speeds) but with the caveat that grid stroke length had to be comparable to the depth of the  
533 tank. As such, Guadayol et al. (2009b) recommended using the maximum stroke length  
534 possible in order to ensure isotropy.

535

### 536 *Vertically oscillating grids*

537 In order to mimic surface layer mixing, grids are typically suspended from the top of  
538 the test tank. Grid nets can be singular (Savidge, 1981) or suspended in series of two or more  
539 grids (Estrada et al., 1987; Alcaraz et al., 1988; Berdalet, 1992). There is also the option of  
540 suspending an inclined, rotating ellipsoidal grid at a specific depth to promote mixing  
541 horizontally as well as vertically (Estrada et al., 1987). While investigating an alternative  
542 method to using grids, a number of disadvantages to using grid systems were identified by  
543 Webster et al. (2004). Having an object moving through the study tank interferes with many

544 direct flow measurement techniques; however indirect techniques, such as particle tracking  
545 velocimetry, can be readily used. Moving grids can also increase the likelihood of mechanical  
546 damage to the study organism. In studies where the grid oscillates in only a small fraction of  
547 the cosm, the turbulence field produced is non-isotropic and directional in accordance with  
548 the direction of the grid motion. In this instance, the turbulence generated is also  
549 heterogeneous as it decays with increasing distance from the grid. Webster et al. (2004) also  
550 cited size, expense and complexity of apparatus as major disadvantages of grid systems; in  
551 reality, however, a simple oscillating grid is vastly simpler than many other turbulence-  
552 generation methods described herein. Furthermore, Warnaaars et al. (2006) recognised that  
553 steep turbulence gradients are typically recorded with grid systems;  $\epsilon$  is highest near the grid  
554 but decays rapidly with distance from the grid. In addition, ancillary flows are seen to  
555 accompany the primary flow field which exposes any test organisms to a wider range of  
556 turbulent regimes than may be desired. Overall, Peters and Redondo (1997) discouraged the  
557 use of oscillating grids on the grounds that the turbulence produced is not properly  
558 representative of naturally occurring turbulence.

559         One disadvantage of grid systems is the steep turbulence gradients found around the  
560 grid itself. If test organisms are permitted in and around the oscillating grid, they not only risk  
561 mechanical destruction but are also exposed to a wider range of  $\epsilon$  than they would in a natural  
562 environment. To prevent organisms from interacting with the region of grid oscillation,  
563 MacKenzie and Kiørboe (1995) used a fine mesh placed below the grid. The study focussed  
564 on swimming behaviour and encounter rates between copepod larvae and cod / herring larvae;  
565 thus, the barrier mesh size was selected to allow the prey copepods to interact with the grid  
566 region while the fish larvae were unable to enter this region. The addition of the mesh screen  
567 is a notable improvement to studies of this nature but could interfere with the turbulent field  
568 produced by the oscillating grid. There is also the possibility that prey could pass through the

569 mesh screen where it could then be subjected to advantageous conditions for increased  
570 growth. The presence of the screen could then prevent the now larger organism from passing  
571 back through the mesh. In the case of phytoplanktonic studies with incident light from above,  
572 this could provide an intrinsic bias to the study.

573

#### 574 *Horizontally oscillating grids*

575 While most practitioners opt for vertically oscillating systems, there are times when a  
576 horizontal system is more suitable. To reduce the likelihood of resuspension of filamentous  
577 and dense species that sediment to the bottom, horizontal grids are better suited if using a  
578 mixed phytoplankton community as shown in a study by Fraisse et al. (2015). Six different  
579 phytoplankton species were selected to represent an array of morphologies (elongated shapes,  
580 flattened shapes and motile species), densities, growth rates and sizes. The study showed that  
581 the species selected that had high sinking rates were unable to outcompete those that could  
582 maintain their positions in the upper column. Similarly, Schapira et al. (2006) made use of  
583 horizontal grid systems taking care to produce both realistic and quantified turbulence  
584 measurements. Opting for low, medium and upper limits of turbulence found in the English  
585 Channel, the researchers investigated the impact of this on the colony-forming dinoflagellate  
586 *Phaeocystis globosa* Scherffel. Results show that turbulence enhanced colony growth and  
587 formation to a threshold amount after which turbulence was found to impede cell growth via a  
588 postulated reduction in cell division (Schapira et al., 2006).

589

#### 590 *Vibrating grids*

591 In addition to oscillating grids, vibrating grids have also been used; to study the effects  
592 of turbulence on zooplankton behaviour, Saiz and Alcaraz (1992) utilised a vertically  
593 orientated grid attached to a vibrating rod which moved the grid in the horizontal axes (x and

594 y). Efforts were made to not only quantify the turbulence generated but to also map the  
595 turbulence field across the tank; it was found that the vertical and horizontal components of  $\varepsilon$   
596 did not differ to any significant extent. The results of the experiment showed that the increase  
597 in turbulence caused a corresponding increase in both copepod suspension and predatory  
598 feeding behaviour thought to result from an increase in predator-prey contact rates (Saiz and  
599 Alcaraz, 1992).

600

#### 601 *Stationary grids*

602         Looking to improve the often-used grid oscillation systems, Warnaars et al. (2006)  
603 used a pair of underwater speakers in anti-phase to push water through a stationary grid  
604 placed directly in front of each speaker. It was observed that the flow characteristic of the  
605 speaker system compared well with grid systems, albeit with lower strain rates making it  
606 more representative of natural turbulence fields. Furthermore,  $\varepsilon$  is seen to attenuate rapidly  
607 with distance from grids in oscillator set-ups; however, the speaker system generated  
608 uniformly distributed  $\varepsilon$  throughout the entire volume of the tank. It is also noted that the range  
609 of turbulence scales observed in grid systems is larger than those measured in the speaker  
610 system; when the chlorophyte *Selenastrum capricornutum* Printz was exposed to the speaker  
611 system, growth rate was seen to increase as conditions became more turbulent. This increase  
612 in growth was attributed to the fact that the range of  $\varepsilon$  experienced by the organisms is more  
613 concurrent with the levels in the natural environment. It should also be noted that in the  
614 absence of a moving grid, this technique permits direct flow velocity measurements. Due to  
615 limitations imposed by equipment practicalities, however, this technique would likely be  
616 restricted to nanocosm and microcosm experiments.

617

618 *Additional case studies*

619 A number of researchers have used similar grid-generated turbulence set-ups to  
620 observe predator-prey interactions within turbulent environments (Peters and Gross, 1994;  
621 Peters et al., 2002; Dolan et al., 2003; Havskum, 2003; Havskum et al., 2005). For example,  
622 Havskum (2003) investigated how grid-generated turbulence affected feeding rates of a  
623 predatory dinoflagellate species linking turbulence to the rate of predator-prey interaction.  
624 The disadvantage of studies of this nature is that, as well as altering the encounter rate, in  
625 many cases the turbulence causes secondary physiological or behavioural changes in the  
626 species studied (e.g., Peters and Gross (1994)). When conducting cosm experiments of this  
627 nature, it is crucial to use planktonic species that are not sensitive to turbulence; for example,  
628 Havskum et al. (2005) observed no change in the autotrophic or mixotrophic growth of the  
629 dinoflagellate *Fragilidium subglobosum* (Stosch) Loeblich III under different turbulence  
630 levels but did observe a change in ingestion rates.

631 In a technique analogous to grid-generated turbulence, Sullivan and Swift (2003) used  
632 a pair of vertically oscillating rods to produce varied intensities of turbulence. Interestingly,  
633 this paper opposed the commonly held view that dinoflagellates as a group are sensitive to  
634 turbulence; out of the 10 species tested, 7 were unaffected by natural levels of turbulence. In a  
635 similar departure from vertically oscillating grids, researchers at the Marine Ecosystem  
636 Research Laboratory (MERL; Rhode Island, USA) mesocosms made use of a rubberised  
637 plunger attached to a vertical pole to simulate tidal mixing. The plunger itself was situated 1m  
638 above the sediment-laden floor to provide realistic levels of tidal sediment resuspension with  
639 the system motor timed to providing a mixing cycle mirroring natural tidal oscillations  
640 (Santschi, 1985).

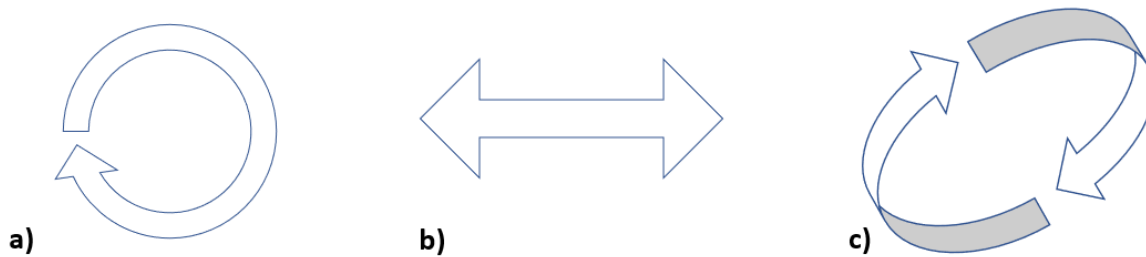
641 Towards the larger scale of mesocosm studies, it is also possible to use grid-generated  
642 turbulence in limnocorrals (Nerheim et al., 2002). Studies undertaken as part of the Nutrients

643 and Pelagic Production project (Nejstgaard et al., 2001b; Nejstgaard et al., 2001a; Nerheim et  
644 al., 2002) encountered difficulties with this approach, however. In order to promote  
645 stratification in some of the limnocorrals, freshwater was added to the surface; this resulted in  
646 the limnocorrals rising up out of the water as the mean internal water density was now lower  
647 than that of the surrounding water. This effect was countered by increasing densities via the  
648 addition of salt to the water in the lower parts of the mesocosms. Altering the salinity to this  
649 extent in a biological study is not advised as this would alter the phytoplankton community in  
650 favour of species that are less sensitive to changes in salinity. Once stratification was  
651 established in the NAPP studies, the grid mixing systems were then used to promote an upper  
652 mixed layer while a low-suction airlift pump system (typically used in aquaculture or marine  
653 archaeology) promoted “slow circulation” in the upper layer.

654

### 655 **Shaker tables**

656 Shaker systems are used across a multitude of sciences for a variety of applications  
657 from agitation of chemicals to the culturing of microbiological organisms. Due to the ubiquity  
658 of shaker tables in academic and scientific institutions, it is not unsurprising that they are  
659 frequently used to generate artificial turbulence. Furthermore, they typically have discrete  
660 settings allowing researchers to generate a broad range of turbulence levels. While some  
661 researchers simply use the rpm settings, more rigorous studies quantify the level of turbulence  
662 via acoustic Doppler velocimetry or similar. It should be noted that specific turbulence flow  
663 patterns generated by shaker tables are difficult to quantify, thus any recorded changes in  
664 biological activity is difficult to ascribe to a particular flow characteristic (Warnaars et al.,  
665 2006). Shaker tables typically use one of three different motion paths depending on their  
666 intended application: orbital or rotary shakers; reciprocal shakers; and, gyratory shakers  
667 (Figure 7).



669

670 *Figure 7 - Motion paths of vessels placed on different types of shaker tables as seen from*  
 671 *above. a) An orbital / rotary shaker oscillates in a circular motion in the x-y plane. b) A*  
 672 *reciprocal shaker oscillates from side to side along a single axis. c) A gyrotory shaker*  
 673 *oscillates vessels in a circular motion with both horizontal and vertical components to the*  
 674 *motion.*  
 675

#### 676 *Orbital shakers*

677       Orbital shakers (a.k.a. rotary shakers) agitate cultures with a circular motion in the x-y  
 678 plane (Figure 7a). Depending on the manufacturer of the shaker, the orbit oscillation is fixed  
 679 at a set distance or can be altered accordingly. Zirbel et al. (2000) used orbital shakers to  
 680 observe changes in dinoflagellate morphology over time. Trials were conducted with the  
 681 shakers set on 40 rpm to 120 rpm before a rate of 75 rpm was designated as “*relatively mild*”  
 682 turbulence. It is noted that for such shaker experiments, turbulence occurs due to wall effects  
 683 within the vessel. This has two ramifications: firstly, the turbulence will increase with  
 684 proximity to the vessel walls and secondly, the vessel needs to be of a suitable size to allow  
 685 turbulent mixing to impact upon fluid in the centre (Peters and Redondo, 1997). Orbital  
 686 shakers typically promote the central “*doldrum,*” or dead-space, region in flasks marked by  
 687 minimal in situ turbulence meaning that the cells are no longer being cultivated under near-  
 688 isotropic conditions (Juhl et al., 2000). Furthermore, the turbulent mixing produced would be  
 689 predominantly horizontal with a weak secondary vertical component. However, horizontal  
 690 eddy diffusivity in the ocean is thought to be “*several orders of magnitude*” greater than the  
 691 vertical equivalent (Okubo (1976) cited in Estrada et al. (1987)).



692 As shaker table experiments typically make use of available apparatus, there is often a  
693 range of different sized and shaped vessels used which makes comparisons between studies  
694 difficult. In a comparative study between turbulence generated by grids versus that generated  
695 by orbital shakers, Guadayol et al. (2009b) trialled a number of different shaker set-ups with  
696 different periods of oscillations as well as various volumes and flask (Florence, Nalgene and  
697 Erlenmeyer) types. The research showed that at high levels of shaking, the turbulence field  
698 remains isotropic independent of volume or flask shape. However, at lower levels of  $\varepsilon$  ( $< 10^{-8}$   
699  $\text{m}^2/\text{s}^3$ ), the isotropy began to fall, probably as a result of lower signal-to-noise ratios (SNR) in  
700 the Doppler velocimeter as well as the fluid approaching the laminar-turbulent transition  
701 point. Furthermore, orbital frequencies of  $< 1$  Hz are not recommended as it is at approximately  
702 this frequency that the laminar-turbulent transition occurs in flasks. As orbital shaker  
703 turbulence is generated via wall friction,  $\varepsilon$  decreases with distance from the sides and bottom;  
704 an order of magnitude decrease in  $\varepsilon$  was observed in measurements when transitioning from  
705 the wall to the centre of the flask. Thus, it is recommended that “*small and narrow*” vessels  
706 (e.g. Nalgene flasks) be used to limit this effect as much as possible (Guadayol et al., 2009b).

707

#### 708 *Reciprocal shakers*

709 Reciprocal shakers oscillate from side to side along a single axis in the x- or y-plane  
710 (Figure 7b). The length along which the oscillation occurs can be altered accordingly with  
711 longer lengths equating to higher levels of turbulence (Juhl et al., 2000). The advantage of  
712 reciprocal shakers is the removal of the central doldrum in the flasks which typically occurs in  
713 orbital shakers. In a comparative study of the effects of shaker-table-generated mixing relative  
714 to Couette-generated shear flow, Juhl et al. (2000) subjected populations of the dinoflagellate  
715 *Lingulodinium polyedra* (F. Stein) J.D. Dodge to different durations of constant mixing.  
716 Actually, reciprocal tables allow standing waves to form in the flask, resulting in an

717 oscillating fluid surface that ensures all cells in the population experience variable mixing.  
718 While the level of turbulence was not quantified directly, attempts were made to approximate  
719 mixing via a comparison of the qualitative outcome between the shaker populations and the  
720 Couette populations; the response of the cells exhibited a similar response in both setups.

721

### 722 *Gyratory shakers*

723 As well as orbital shakers and reciprocal shakers, there are also gyratory shakers  
724 which oscillate vessels in a circular motion with both horizontal and vertical components to  
725 the motion (Figure 7c). An experiment was carried out to observe effects of gyratory-shaker-  
726 generated turbulence (as well as of growth medium, fluid depth, tank material and initial cell  
727 concentration) on the doubling time of the protozoan *Tetrahymena* sp. (Hellung-Larsen and  
728 Lyhne, 1992). It was noted that gyrational shaking resulted in a circular wave that propagated  
729 around the edge of the shaking vessel. The study showed that the doubling time was increased  
730 (i.e., cell division decreased) with shaking but the impact of the shaking reduced with  
731 increased fluid depth. Morphologically, cells that were exposed to shaking exhibited less-  
732 prominent nuclear membranes and the development of small granules inside the cell  
733 cytoplasm. It was also observed that viscosity played a role as the effect of shaking on cell  
734 division was reduced when dextrane was added to increase the viscosity of the medium;  
735 clearly, the increase in viscosity acted to reduce the overall level of turbulence in the vessels.  
736 The study also compared the impact of gyratory agitation to reciprocal shaking and bubbling;  
737 when using gyrational shaking, the impact of shaking rate on cell division was seen to be  
738 dependent on initial cell concentration, but this was not so for reciprocal shakers  
739 (Hellung-Larsen and Lyhne, 1992).

740

741 *Additional case studies*

742 Building upon early work regarding the mass culture of algae, Fogg and Than-Tun  
743 (1960) used a shaker apparatus to ascertain the optimum shaking speed to maximise cultures  
744 of *Anabaena cylindrica* Lemmermann. Even low agitation speeds were seen to increase cell  
745 growth compared to unshaken cultures. While moderate shaking was seen to increase growth  
746 due to increased suspension and nutrient flux, if the shaking rate exceeded 140 rpm, the cell  
747 growth rate showed no increase when compared to unshaken cultures. Opposing these  
748 findings, Tuttle and Loeblich (1975) attempted to find the optimal growth conditions for the  
749 dinoflagellate *Cryptocodinium cohnii* (Seligo) Chatton and observed exponential death rates  
750 of cells at both 40 and 80 rpm; these early results hinted at the turbulence sensitivity of some  
751 dinoflagellate species.

752 In what has now become a classic paper in the study of phytoplankton-turbulence  
753 interaction, White (1976) used rotary shakers to agitate cultures of *Alexandrium tamarense*  
754 (Lebour) Balech to note the effect on cell growth while investigating the cause of red tides in  
755 Eastern Canada. Results show that cell growth reduced rapidly at high levels of continuous  
756 shaking; even intermittent shaking and/or shaking at low speeds was seen to adversely affect  
757 cell growth. As well as mechanical destruction, White (1976) attributed the decreased growth  
758 rate to cell disorientation that caused subsequent interference with phototactic migration.  
759 Peters and Marrasé (2000) have since estimated the turbulence generated in this study to be  
760 higher than natural  $\varepsilon$  with values between  $4.30 \times 10^{-3}$  and  $1.19 \times 10^{-2} \text{ m}^2/\text{s}^3$ . While the White  
761 (1976) study made no attempt at turbulence quantification (it was, after all, at the time seen as  
762 a purely biological study), it none-the-less sparked interest in turbulence studies within the  
763 marine ecological community.

764 Clearly drawing upon these findings, Berdalet (1992) sought to identify the  
765 mechanism(s) by which cell growth is reduced in turbulence. Cultures of the HAB

766 dinoflagellate *Akashiwo sanguinea* (K. Hirasaka) Gert Hansen & Moestrup were exposed to  
767 shaker-table turbulence with cellular volume, shape and location of nuclei, RNA and DNA  
768 concentrations all recorded. Berdalet (1992) postulated that the observed reduction in growth  
769 was a result of the physical disruption of chromosome separation during cell division. Again  $\varepsilon$   
770 was unquantified in this study (Peters and Marrasé (2000) later estimated the corresponding  $\varepsilon$   
771 as  $2 \times 10^{-3} \text{ m}^2/\text{s}^3$ ), but more recent studies based on the same experimental set-up utilised an  
772 acoustic Doppler velocimeter to record water speed at different points in the flask (Berdalet et  
773 al., 2007). Of relevance within the current review is a thorough literature overview of all  
774 experiments on turbulence-dinoflagellate interactions which, as per Peters and Marrasé  
775 (2000), includes estimates for  $\varepsilon$  calculated using experimental set-up data from individual  
776 experiments (see Appendix 3).

777

## 778 **Aeration systems**

779 When biologists look to cultivate cells, they often seek to aerate the water via a bubble  
780 stone at the base of the tank which allows gases (e.g., CO<sub>2</sub>, oxygen) to diffuse into the water,  
781 promoting growth. As such, bubble plumes and aeration systems in the lab are a tried and  
782 tested technique for mixing water and aerating growth tanks. Furthermore, most  
783 microbiological laboratories have access to air compressors and piping to facilitate the use of  
784 aeration systems. A by-product of this aeration is that the bubbles themselves break down any  
785 stratification, thereby homogenising the water while also advecting the cells as the central  
786 bubble plume effectively promotes formation of a toroidal convection cell in the tank. Within  
787 the mesocosm community, aeration systems are typically seen to be gentler in their approach  
788 to turbulence generation due to their absence of moving parts that have the potential to  
789 mechanically damage organisms (Sanford, 1997; Striebel et al., 2013).

790 In laboratory setups, it can be difficult to determine whether the change in growth rate is  
791 a result of the turbulence induced by the bubble flow or as a result of atmospheric gases being  
792 entrained through the water. How the culture will react is species-dependent with dissolved  
793 oxygen being required for respiration while CO<sub>2</sub> promotes photosynthesis. Gas addition can  
794 also result in a change in pH via CO<sub>2</sub>-induced decreases in the pH of water; this can have  
795 impacts for pH-sensitive species (Havskum and Hansen, 2006). An unintended side-effect of  
796 bubbler aeration systems is a temperature change to the fluid medium. As gases that are  
797 introduced to the fluid are typically at air temperature, this can impart additional thermal  
798 energy to the system. Furthermore, as the gas has typically undergone pressurisation prior to  
799 release, there may also be associated adiabatic thermal effects.

800 Båmstedt and Larsson (2018) noticed an aggregation of bacteria, algae and detritus at  
801 the water surface of their unmixed cosms during experiments. This was thought to be the  
802 result of surface heating from the overhead irradiance lamps causing a thermal lid effect in the  
803 upper 60 cm. It was found that bubbling at a rate of 1 Hz from 2 cm depth was sufficient to  
804 break up the surface aggregation, but some mixing was required to break the thermal lid. As  
805 such, a comparison between bubbling and surface mixing using fans angled at 45° to the  
806 surface was carried out; overall fan mixing was found to mix the mesocosm faster than  
807 bubbling. It should be taken into consideration that the bubbler system was set to emit a single  
808 18 mm-diameter bubble at 1 Hz so as to not cause any undesirable aeration effects.

809 In an attempt to determine the optimal conditions for cultivating the dinoflagellate  
810 *Cryptothecodinium cohnii*, Tuttle and Loeblich (1975) subjected cultures of cells to agitation by  
811 aeration (as well as magnetic stirrers and shaker tables). Sterilized air was bubbled through  
812 the medium at a rate of 1.8 L/min; the increase in observed growth rate was negligible. In a  
813 series of experiments exploring potential biomass species, Thomas et al. (1984a); Thomas et  
814 al. (1984b); Thomas et al. (1984c) used aeration systems to “vigorously” aerate and mix the

815 cell cultures. Using a gas mix of 1% CO<sub>2</sub> in air, two aeration pipes were placed at the bottom  
816 of the tank and gas supplied at a rate of 2000 ml/min. The researchers reported “very high  
817 densities” and reported no evidence of mechanical damaging of the cells despite the high  
818 aeration rate. There was no control tank setup nor any attempt to quantify the turbulence  
819 produced. Again, with reference to the commercial cultivation of phytoplankton, Aguilera et  
820 al. (1994) used bubbler agitation in chemostats to mix cultures of a microalga. Novel in this  
821 experiment was an attempt to quantify mixing in terms of mechanical energy supplied to the  
822 system calculated using standard physical equations relating gas pressure, velocity, and the  
823 conservation of mass and/or energy. Within this work, the role of turbulence was recognised  
824 in preventing sedimentation, promoting a homogenous distribution of cells and nutrients, and  
825 increasing the nutrient supply to the surface of the cell. However, agitation by bubbles was  
826 also cited as a way by which gases are more efficiently diffused into the medium. As  
827 discussed earlier, this effect of increased gas diffusion on cell growth would be difficult to  
828 distinguish from changes due to the increase in turbulence.

829         Aeration systems have been used to good effect for studying natural planktonic  
830 communities (Eppley et al., 1978; Sonntag and Parsons, 1979). As part of the Controlled  
831 Ecosystem Pollution Experiment (CEPEX), Sonntag and Parsons (1979) used aeration to  
832 simulate upwelling, then added salmonids to create an additional trophic layer that would  
833 ordinarily be absent (the enclosures were taken to depth by divers and then slowly raised so  
834 any suitably motile organism would have been able to escape). The study recorded high rates  
835 of phytoplankton sedimentation suggesting that the aeration regime chosen was insufficient to  
836 promote resuspension. Using the same limnocorrals, Nerheim et al. (2002) combined grid-  
837 generated turbulence with an aeration system to study a natural food web. Researchers  
838 quantified the rate of vertical mixing via a dye dispersion study; this led them to realise that  
839 the vertical eddy diffusivity was 0.06 cm<sup>2</sup>/s, lower than the expected value outside of the

840 enclosures (Steele et al., 1977). It was thus postulated that the presence of the enclosures  
841 reduced the horizontal mixing and as this is coupled to vertical mixing, there was a  
842 subsequent impact on vertical mixing also. Efforts were made to limit daily mixing to the  
843 level just required to break any measured stratification; however, no efforts were made to  
844 quantify this vertical mixing. Microscopic analysis of the species within the enclosures  
845 verified that the bubbles did not damage cells mechanically, with Eppley et al. (1978)  
846 reporting “no grossly unnatural results”.

847

### 848 **Couette cylinders**

849       Named after French physicist Maurice Couette who first used them in 1890 (Couette,  
850 1890), this equipment generates shear flow in a small gap between two concentric cylinders.  
851 A fluid medium is placed in the gap between the smaller inner cylinder and the larger outer  
852 cylinder. The inner cylinder then rotates at a given speed producing uniform flow conditions  
853 (Peters and Redondo, 1997; Sullivan and Swift, 2003). A key advantage of this setup is that  
854 shear flow can be easily calculated from angular velocity, thereby removing the need for  
855 physical measurements to calculate flow parameters. Furthermore, a variety of different forms  
856 of turbulence can be produced by rotating the cylinders at different velocities relative to each  
857 other. However, Sullivan and Swift (2003) reported that the turbulence produced by Couette  
858 cylinders is intrinsically unrepresentative of natural turbulence because it applies constant  
859 shear both temporally and spatially.

860       Some of the first phytoplankton-turbulence studies were carried out using Couette  
861 cylinders. Pasciak and Gavis (1975) conducted a series of experiments on the effect of  
862 turbulence on nutrient uptake rate in diatoms. Interestingly, they compared the uptake rate  
863 between cell cultures on orbital shaker tables to those inside a Couette flow. While the shear  
864 flow rate was calculated for the Couette flow, no attempt was made to quantify the turbulence

865 generated inside the flasks on the shaker table. Building upon this work, Thomas and Gibson  
866 (1990a,b) used an almost identical set-up to observe the impact of shear flow on nutrient  
867 uptake on *Lingulodinium polyedra*, a HAB-forming dinoflagellate species. Using a series of  
868 Couette cylinders with rotational speeds ranging from 1 rpm up to 60 rpm, the researchers  
869 calculated various turbulent parameters using the rotational speed.

870         Using a similar Couette set-up, Juhl et al. (2000) also conducted an investigation on  
871 the dinoflagellate, *Lingulodinium polyedra*. The aim of this experiment was to account for the  
872 variability in studies by measuring the effect of turbulence on population growth under  
873 varying light-dark cycles, differing light levels and different stages of the cell cycle. The  
874 outcomes highlighted a number of key mechanisms: a) that cell growth rate decreased more  
875 when flow was applied in the last hour of the dark phase as compared to applying it to  
876 illuminated cultures; b) populations cultured in lower light conditions experienced  
877 proportionately lower growth rates when exposed to flow than those cultured in higher light  
878 conditions and c) older cultures in the late exponential phase experience higher mortality  
879 under flow than cells in the early phase. A key outcome of this study was that the extent to  
880 which turbulence affects the cell population is not only light-dependent but also depends on  
881 the physiological state of the cell (and the phase of its life cycle).

882 Juhl et al. (2000) also compared the outcomes of the Couette studies to equivalents carried out  
883 using turbulence generated using shaker tables. Unfortunately, the shaker table turbulence  
884 was unquantified; however, attempts were made to approximate the shear flow via a  
885 qualitative comparison of results. It should be noted that Warnars et al. (2006) recognised  
886 that the minimum strain rate used in the studies of Thomas and Gibson (1990a,b) were up to  
887 two orders of magnitude greater than those observed in the natural environment.

888



889 A summary of turbulence generation methods and associated advantages and  
890 disadvantages can be found in Table 3, along with example references highlighting best  
891 practice for each of the main techniques. Based on this review, it is recommended that  
892 oscillating grids become the turbulence-generation standard; of the techniques evaluated, the  
893 grid-generated turbulence is closest to that found in natural systems. Furthermore, it is  
894 relatively easy to adjust the experimental set-up in order to facilitate species across different  
895 groups and, on a broader topic scale, across the different marine science sub-disciplines. This  
896 technique is also the most commonly used (

897 Table 1), thereby facilitating easy comparisons with any future study. See Appendix 1  
898 for a summary of lesser-used techniques for generating turbulence including pumping,  
899 magnetic stirrers, rotating chambers, wave tanks, impellers / propellers, paddles, dialysis  
900 cylinders and convective mixing.

901

902 *Table 3 - Summary table of commonly used turbulence generation techniques*

<b>Technique</b>	<b>Pro</b>	<b>Con</b>	<b>Example</b>
<b>Oscillating Grids</b>	<ul style="list-style-type: none"> <li>• Can be configured for near-isotropic turbulence</li> <li>• Reduction in resuspension (horizontal grids)</li> <li>• Can use mesh screens to create refuge area</li> </ul>	<ul style="list-style-type: none"> <li>• Obstructs flow velocity measurement equipment</li> <li>• Risk of mechanical damage to organisms</li> <li>• Steep turbulence gradients; <math>\epsilon</math> highest near grid but decays rapidly with distance</li> </ul>	Schapira et al. (2006)
<b>Shaker tables</b>	<ul style="list-style-type: none"> <li>• Low-cost, off-the-shelf equipment</li> <li>• Commonly found in laboratories</li> </ul>	<ul style="list-style-type: none"> <li>• Typically restricted to small volumes</li> <li>• Turbulence generated is non-isotropic with high <math>\epsilon</math> near flask wall decreasing towards centre</li> </ul>	Berdalet et al. (2007)
<b>Aeration systems</b>	<ul style="list-style-type: none"> <li>• Can be applied across all scales of cosm</li> <li>• Commonly found in microbiological laboratories</li> </ul>	<ul style="list-style-type: none"> <li>• Introduction of gases causing secondary growth effects in cells</li> <li>• Bubbles can cause adiabatic thermal effects and impede flow velocity measurements</li> </ul>	Aguilera et al. (1994)

	<ul style="list-style-type: none"> <li>• Possible to use equations to estimate turbulence from energy input</li> </ul>	<ul style="list-style-type: none"> <li>• Not quantifiable turbulence</li> </ul>	
<b>Couette cylinders</b>	<ul style="list-style-type: none"> <li>• Shear flow can be calculated from angular velocity, removing the need for physical measurements</li> </ul>	<ul style="list-style-type: none"> <li>• Turbulence unrepresentative of natural systems</li> </ul>	Stoecker et al. (2006)

903

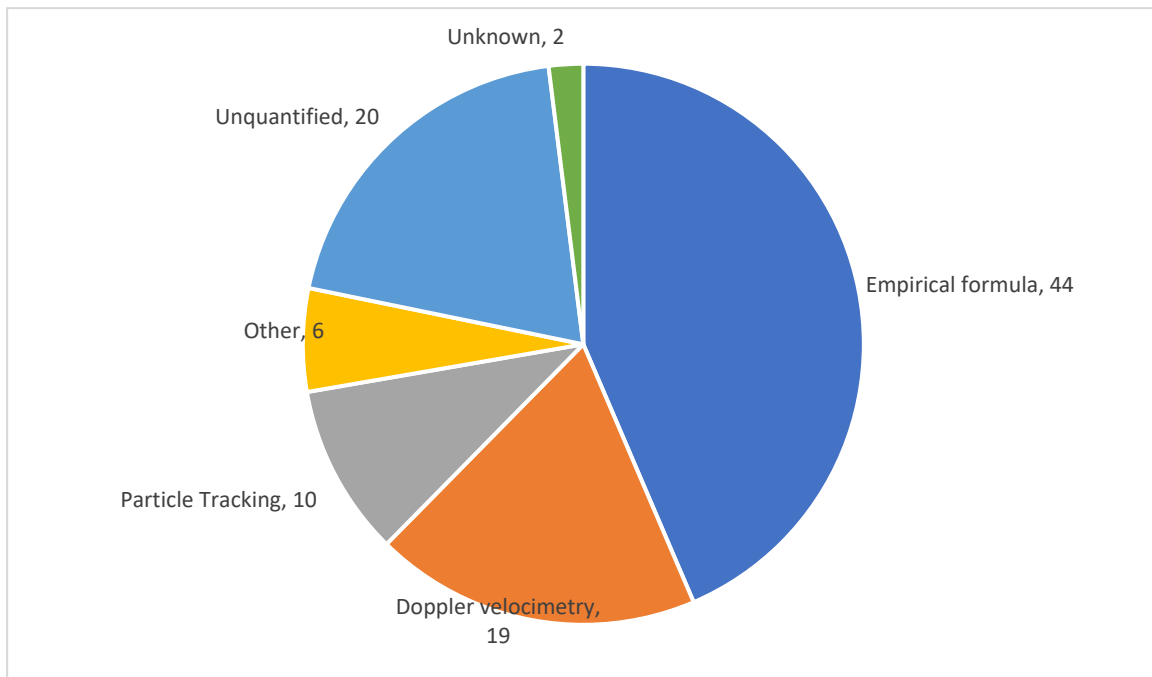
904

905 **METHODS FOR QUANTIFYING TURBULENCE**

906 It is crucial to properly describe the nature and quantify the magnitude of the turbulent  
907 environment within a cosm. To relate a cosm experiment back to its intended real-world  
908 application, organisms should be exposed to turbulence that mirrors natural turbulence as  
909 closely as possible. While some studies simply use the rate of motor revolutions as a proxy  
910 for turbulence quantification, others use an array of techniques to maintain turbulence  
911 requirements. It should be noted that a majority of turbulence-generation techniques involve  
912 the placement of movement apparatus in the test tanks (e.g., grids); as a result, it becomes  
913 difficult to place sensors for turbulence measurement undisturbed in the tank as well.

914 Instead of measuring turbulence directly, some researchers simply consider the  
915 mechanical energy input to the cosm (Kiørboe et al., 1990; Aguilera et al., 1994; Martínez et  
916 al., 2017). For example, in a grid-generated turbulence study, Kiørboe et al. (1990) was able  
917 to calculate  $\varepsilon$  as a function of power input from the motor as  $\varepsilon = W/V \times 1/\rho$ , where  $W =$   
918 power input (W),  $V =$  volume of fluid ( $m^3$ ) and  $\rho =$  density of fluid ( $kg/m^3$ ). While easily  
919 calculated, these values are often theoretical and can be presented without proper calibration.  
920 Given the ad hoc nature of many turbulence experiments, this estimate of  $\varepsilon$  (and associated  
921 calibration) must be considered on a case-by-case basis (Guadayol et al., 2009b).  
922 Furthermore, it also makes comparison between different studies difficult as this  $\varepsilon$  value is not  
923 standardised nor easily comparable to natural systems.

924 The following section provides an overview to the various techniques used to quantify  
925 turbulence as well as any corresponding advantages and/or disadvantages. Methods reviewed  
926 include particle tracking velocimetry, particle imaging velocimetry, planar laser induced  
927 fluorescence, Doppler velocimetry, and calculation via empirical formulae. Figure 8 shows a  
928 breakdown of how frequently various methods have been used for turbulence quantification.  
929



930

931 *Figure 8 – Methods used to quantify turbulence in the publications reviewed. Particle*  
 932 *tracking: refers to particle tracking velocimetry, DPIV and PLIF. Doppler velocimetry: refers*  
 933 *to ADV and LDV. Other: refers to dye dispersion and bioluminescence.*

934

### 935 **Particle tracking velocimetry**

936 As a precursor to digital image analysis techniques, early particle imaging was carried

937 out using video recorders attached to microscopes (e.g. Saiz and Alcaraz (1992)). This

938 technique involves the direct imaging of individual tracer particles (e.g., reflective spheres or

939 phytoplankton cells) highlighted by a sheet of laser light. An image is taken and compared to

940 another image taken some small time period later. The subsequent direct image comparison

941 allows for local particle displacement to be determined. By accounting for the time delay and

942 image magnification, it is possible to map the velocity field of a tank. While this analysis has

943 proven to be computationally expensive, it does result in a high vector density with good

944 accuracy and spatial resolution (Webster et al., 2001). The image field is then divided into a

945 grid, the instantaneous velocities are decomposed into horizontal and vertical components, the

946 spatial means within a grid cell are computed. This spatial mean is then subtracted from the

947 instantaneous velocity field to yield the fluctuating component of the particle velocities,

948 which is representative of the turbulence in the flow, and, from this, the turbulent dissipation  
949 rate can be determined (Marrasé et al., 1990; Saiz and Alcaraz, 1992).

950 Technological advances in velocimetry are now permitting fluid dynamicists to  
951 measure the flow fields across illuminated planes within a cosm. As water is a transparent  
952 medium, these techniques typically involve the illumination of particles suspended in the  
953 fluid, as suspended sediment, planktonic organisms or artificially introduced reflective  
954 particles. These particle tracking velocimetry techniques typically involve an external source  
955 of illumination (e.g., a light or laser) and an external camera. Thus, a benefit of these  
956 techniques is that they do not require apparatus to be placed in the test tank; hence, they can  
957 be used with a variety of turbulence-generation methods. While advances in particle tracking  
958 velocimetry now permit detailed imaging of 3D flows (Hoyer et al., 2005; Raffel et al., 2018),  
959 this has yet to be applied to any bio-turbulence studies which, to date, have not progressed  
960 beyond two-dimensional (2D) imaging. This technique is sometimes referred to as digital  
961 particle tracking velocimetry (DPTV) (Webster et al. (2001).

962

### 963 **Digital Particle Imaging Velocimetry**

964 Digital particle imaging velocimetry (Digital PIV or DPIV) involves seeding the test  
965 fluid with highly reflective neutrally buoyant particles. The size of the particles required is  
966 dependent on the size of the fluid structures required by the study. A laser light sheet is then  
967 projected into the tank resulting in an illuminated plane. This laser is synchronised to a digital  
968 camera positioned perpendicular to the illuminated plane which photographs the particle  
969 movement; this allows a velocity map of fluid motion to be produced. It is important to select  
970 a suitable laser pulse and shutter speed to prevent signal distortion and other artefacts (Zirbel  
971 et al., 2000). Older DPIV systems required the simultaneous use of two digital camera and  
972 corresponding laser sheets to image 3D flow; this required unimpeded access to different

973 sides of the cosm (Eder et al., 2001). Fortunately, more modern techniques (e.g., tomographic  
974 PIV; tomo-PIV) have streamlined the measurement of 3D and time-resolved (four-  
975 dimensional) flows with both overall precision and higher spatial resolution (Scarano, 2012;  
976 Raffel et al., 2018). Calculation of  $\varepsilon$  using PIV can be a mathematically complex procedure.  
977 Assuming the turbulence is both isotropic and homogeneous, Xu and Chen (2013) simplify  
978 the estimation of  $\varepsilon$ :

$$979 \quad \varepsilon = 15\nu \left\langle \left( \frac{\partial u'}{\partial x} \right)^2 \right\rangle \quad (1)$$

980 where  $\langle \cdot \rangle$  denotes a mean average,  $\nu$  = kinematic viscosity (m<sup>2</sup>/s), and  $u'$  = velocity  
981 fluctuations in the x direction with  $u' \equiv u - \langle u \rangle$  and  $u$  being the x-component velocity (m/s).

982         The introduction of lights and lasers into the fluid medium does have the potential to  
983 influence the behaviour of the test organisms. Phototaxic phytoplankton species that use light  
984 to orientate their swimming direction could be drawn towards the laser light. Furthermore,  
985 high-intensity lasers could in theory cause photo-inhibition in photosynthetic organisms and  
986 reduce the rate of primary production. Motile phototactic species could also be influenced;  
987 however, Linares (2015) observed in a turbulence experiment designed to specifically study  
988 the potential for laser-induced photoinhibition, that “laser exposure has little effect on  
989 phytoplankton”.

990         While it is standard practice to add tracer particles to the test medium to increase the  
991 SNR (Estrada et al., 1987; Fraisse et al., 2015), it is important to select an appropriate tracer.  
992 The motion of any tracer is assumed to follow the flow dynamics of a setup; the extent to  
993 which the tracer particles accurately follow the flow can be determined via the Stokes  
994 number. The test tracer should have a Stokes number  $\ll 1$  in order for the tracers to mirror  
995 the fluid movement; a Stokes number  $< 0.1$  will ensure an accuracy of 99% (Tropea and  
996 Yarin, 2007). A tracer should also be neutrally buoyant and sized appropriately; a smaller

997 diameter is preferable but should be large enough to be recorded. The tracer selected should  
998 be reflective so as to scatter the incident laser light; Webster et al. (2001) reported titanium  
999 dioxide particles have a superior reflectance to comparably sized nylon bead tracers or kaolin.  
1000 Organic substances such as *Lycopodium* pollen grains (Saiz and Kiørboe, 1995) and rheostatic  
1001 fluid (made from fish scales (Latz et al., 1994; Hondzo et al., 1997) can also be used as  
1002 tracers, though the addition of extra organic matter and its subsequent decomposition could  
1003 influence growth rates. As such, tracers are normally added to cosms absent of test organisms.  
1004 If a tracer is added to a tank containing organisms, it should be both non-toxic and non-  
1005 influential on growth rates. For environmental reasons, it is prudent to avoid the use of  
1006 microplastics; if the chosen tracer is a plastic, the particles should be recovered before  
1007 disposal.

1008

### 1009 **Planar Laser Induced Fluorescence**

1010 PLIF is similar to DPIV but makes specific use of the fluorescent properties of  
1011 phytoplankton. As with DPIV, a laser sheet is introduced into the fluid medium to illuminate  
1012 a 2D cross-section with the cosm. Phytoplankton cells are seen to have inherent fluorescent  
1013 properties due to the presence of chlorophyll compounds and other photosynthetic cellular  
1014 organelles. As such, phytoplankton cells are known to exhibit a peak absorption wavelength  
1015 of light at ~440 nm. Following absorption, the light is subsequently re-emitted as a lower  
1016 energy photon at ~685 nm manifesting itself as fluorescence (Leeuw et al., 2013). It is  
1017 possible to calibrate this fluorescence intensity to attain cell concentration as well as directly  
1018 measure the velocities of individual cells akin to DPIV (Liu et al., 2017). Interestingly, as  
1019 technology has progressed the robustness of PLIF systems has increased to the point where  
1020 these systems can be deployed directly in the field, allowing researchers to obtain in situ  
1021 measurements on fluorescent particle distributions (Franks and Jaffe, 2008). As an extension

1022 of PLIF, 3D laser induced fluorescence (3D LIF) technology exists that is able to reconstruct  
1023 a 3D frozen-field image of a fluid flow by scanning perpendicular to the 2D laser sheet  
1024 (Crimaldi, 2008); to date, no evidence could be found of it being applied to bio-turbulence  
1025 studies. Despite the differences in technology, quantification of turbulence based on DPIV  
1026 and PLIF draws upon the same calculations.

1027 Relying on fluorescence does mean that any other photo-active particles and/or  
1028 chemicals in the fluid medium will obscure the fluorescent signature. In particular, the  
1029 presence of CDOM can preferentially absorb certain light wavelengths and attenuate light  
1030 transmission through the water. The fluorescence intensity from certain dyes are also  
1031 dependent on the pH and temperature of the water (Crimaldi, 2008), so this should be  
1032 corrected for to allow comparisons between studies. Also of note is the process of  
1033 photobleaching by which the fluorescent intensity of a dye or phytoplankton cell diminishes  
1034 over time with prolonged exposure to high-intensity light of certain wavelengths; selection of  
1035 a suitable dye should prohibit these effects but dyes that are less susceptible to photobleaching  
1036 are typically more costly (Crimaldi, 2008).

1037

### 1038 **Doppler velocimetry**

1039 Doppler velocimetry involves introducing a soundwave or laser of known frequency  
1040 into a fluid medium. This beam is then reflected off moving particles within the fluid causing  
1041 a measurable frequency shift. Doppler velocimetry allows the user to accurately measure 3D  
1042 mm-scale velocities within a water body.

1043

#### 1044 *Acoustic Doppler Velocimetry*

1045 Single-point velocity Acoustic Doppler Velocimeters (ADV) can be used to good  
1046 effect to measure 3D point velocities. As the name would suggest, ADVs utilise the Doppler



1047 effect by which a pulse of sound of a known frequency is sent into the water from a central  
1048 transducer. This pulse is reflected by particles in the water back to three receivers which  
1049 calculate the motion of the water from the shifted frequency. The reflective particles in the  
1050 water can be natural (e.g., sediment, microorganisms) or artificial (e.g., seeded particles in test  
1051 tanks). The addition of such particles greatly improves the SNR, which is especially useful in  
1052 quiescent flows.

1053         While the resolution of the instrument varies with manufacturer (as well as sampling  
1054 rate and sampling volume), one can directly quantify different turbulence parameters with  
1055 suitable processing by measuring Reynolds stresses (Lohrmann et al., 1995) or by fitting the  
1056 Kolmogorov  $-5/3$  slope to the inertial subrange of the velocity spectra (Bluteau et al., 2011).  
1057 ADVs have many logistical advantages; namely, they provide a relatively simple and  
1058 inexpensive way to quantify turbulence (Bluteau et al., 2011) while also being portable and  
1059 robust. Furthermore, they do not require frequent calibration and are not constrained by  
1060 turbidity as optical sensors are (Lohrmann et al., 1995). As well as bio-turbulence studies,  
1061 ADVs are commonly used as velocity sensors in physical limnological and oceanographic  
1062 studies both in the laboratory and in the field.

1063         Building upon a previous study that overlooked the quantification of turbulence  
1064 (Berdalet, 1992), Berdalet et al. (2007) used a side-mounted Nortek 3D 10 MHz ADV to  
1065 record current velocities at different points within a test flask placed on a shaker table.  
1066 Interestingly, the ADV was mounted on the shaker table so was stationary relative to the  
1067 flask. Sullivan and Swift (2003) used a Sontek ADV to quantify  $\varepsilon$  at different positions across  
1068 a range of turbulent intensities. As with DPIV, the test medium was also seeded with  
1069 microparticles in order to increase the acoustic backscatter and thus improve the SNR.  
1070 Sullivan and Swift (2003) used two different mathematical techniques to calculate turbulence  
1071 from the velocity measurements, providing a comparison of values which showed that the two

1072 methods yielded similar results. These researchers went to lengths to ensure that the levels of  
1073 turbulence generated in the experiments were analogous to those found in the ocean (namely,  
1074  $\varepsilon = 10^{-8} \text{ m}^2 \cdot \text{s}^{-3}$  for the lower turbulence level and  $\varepsilon = 10^{-4} \text{ m}^2 \cdot \text{s}^{-3}$  for the higher) and compared  
1075 them to published  $\varepsilon$  values. A Nortek ADV was used by Guadayol et al. (2009b) to assess the  
1076 differences in  $\varepsilon$  between grid- and shaker-generated turbulence. Depending on the  
1077 manufacturer, the pronged head of an ADV can have a maximum diameter  $\sim 10\text{cm}$  in diameter  
1078 thus limiting the size and shape of vessel in which it is possible to obtain measurements. In  
1079 order to record the velocity in a small grid-generated turbulence vessel, this study made use of  
1080 a set of bespoke 2 L and 15 L vessels that incorporated the transducer heads into the wall of  
1081 the vessel itself. The vessels were constructed from Delrin plastic to limit the internal  
1082 reflection from the tank walls. A larger 2500 L mesocosm tank was constructed with a grid of  
1083 mesh size 10 cm so that the ADV could be deployed through the mesh without interfering  
1084 with the grid mechanism. With regards to measuring velocities in the orbital shaker vessels, a  
1085 custom-made, side-looking ADV was placed in the vessel, held in place by a posable arm also  
1086 attached to the shaker as per Berdalet et al. (2007). Also of interest in these studies is the  
1087 sampling time requirements; a longer sampling time is needed in larger vessels to resolve  
1088 larger overturns. Thus, a minimum duration of 10 minutes was used in the grid tanks and 5  
1089 minutes for the shaker tables.

1090

### 1091 *Laser Doppler Velocimetry*

1092       Optical Laser Doppler Velocimeters (LDV) can be used in a manner similar to  
1093 acoustic Doppler velocimetry. The fluid medium is seeded with reflective beads in order to  
1094 increase the SNR and then the laser is used to image particle motion within the fluid.  
1095 Usefully, the technology has now advanced to the point where it is now readily commercially  
1096 available with an easy installation. Unlike DPIV, only a single system is need to image 3D

1097 flows (Eder et al., 2001). Due to the use of lasers and seeded water, this method has been  
1098 incorrectly referred to as DPIV in some literature; however, similar considerations regarding  
1099 the introduction of laser beams to water and the addition of seeded particles discussed should  
1100 be applied.

1101         In situations where it is difficult to place the sensor in the tank directly (due to size or  
1102 presence of other apparatus), it is possible to image the fluid motion from outside the tank if  
1103 the vessel is transparent and taking into account any inherent refractive effects. Peters and  
1104 Gross (1994) mitigated this lensing effect by constructing a replica test tank solely for  
1105 turbulence quantification. The replica tank was built out of transparent acrylic; it was  
1106 surrounded by a second, square acrylic tank which was then filled with water. The outer layer  
1107 of water surrounding the test tank reduced the ratio of refractive indices, thereby reducing the  
1108 effects of refraction. The test tank was seeded with rutile (a mineral of titanium oxide) spheres  
1109 of 2 to 3  $\mu\text{m}$  diameter and particle velocities were measured in the  $u$  and  $v$  directions via a 2-  
1110 axis laser anemometer.

1111         A summary of the pros and cons associated with each method discussed in this section  
1112 can be found in Table 4.

1113

1114

1115 *Table 4 - Summary table of different turbulence measurement techniques*

<b>Technique</b>	<b>Pro</b>	<b>Con</b>
<b>Particle tracking velocimetry</b>	<ul style="list-style-type: none"> <li>•High accuracy and spatial resolution</li> <li>•External to tank</li> </ul>	<ul style="list-style-type: none"> <li>•Redundant technology with the advent of more powerful CPUs and digital cameras</li> </ul>
<b>DPIV</b>	<ul style="list-style-type: none"> <li>•External to tank</li> <li>•Produces velocity fields over the full field of view of the camera</li> </ul>	<ul style="list-style-type: none"> <li>• Can be difficult to set up</li> <li>•Equipment set-up can be very costly</li> <li>•Potential for introduction of microplastics into water ways</li> <li>•Refraction effects need to be accounted for</li> <li>•Requires access to the tank from at least two directions</li> <li>•Requires two sets of equipment to visualise flows in 3D</li> <li>•Complex, highly technical experimental set-up</li> </ul>
<b>PLIF</b>	<ul style="list-style-type: none"> <li>•Can map cell concentrations as well as velocities</li> <li>•Can be deployed in the field in situ</li> <li>•External to tank</li> <li>•Produces velocity fields over the full field of view of the camera</li> </ul>	<ul style="list-style-type: none"> <li>• Can cause photobleaching in cells</li> <li>•Refraction effects need to be accounted for</li> <li>•Complex, highly technical experimental set-up</li> </ul>
<b>ADV</b>	<ul style="list-style-type: none"> <li>•Portable and robust</li> <li>•Can be used in turbid water</li> <li>•Possible to obtain multiple turbulence characteristics</li> </ul>	<ul style="list-style-type: none"> <li>•Difficult to use in tanks with moving parts</li> <li>•Only point measurements</li> </ul>
<b>LDV</b>	<ul style="list-style-type: none"> <li>•Simple installation and use</li> <li>•External to tank</li> </ul>	<ul style="list-style-type: none"> <li>•Refraction effects need to be accounted for</li> <li>•Equipment set-up can be very costly</li> <li>•Potential for introduction of microplastics into water ways</li> <li>•Only point measurements</li> </ul>

1116

1117 **Empirical formulae**

1118 Empirically derived formulae are used in 44% of publications to quantify turbulence  
 1119 (Figure 8), reflecting the high proportion of studies using Couette cylinders and shaker tables.  
 1120 In circumstances where the cosm is either too small or unsuitable to use measurement  
 1121 apparatus, it is possible to approximate the level of turbulent intensity using basic

1122 measurements of the experimental set-up. This may be useful for researchers that do not have  
1123 access to the high-cost, specialist measurement apparatus discussed previously. It is  
1124 recommended to report turbulence quantification as dissipation rates ( $\epsilon$ ;  $\text{m}^2/\text{s}^3$ ) to be  
1125 concurrent with physical oceanographic observations in the field and thus facilitate  
1126 comparison between studies. As such, Equations (3) and (5) below have been modified to  
1127 output in  $\text{m}^2/\text{s}^3$ .

1128

1129 *Shakers*

1130 Due to their small size and vessel motion, shaker experiments have typically  
1131 precluded direct fluid measurement (the exception being Zirbel et al. (2000) who used PIV).  
1132 As such, Peters and Marrasé (2000) were able to retrospectively estimate  $\epsilon$  in a number of  
1133 studies:

1134

1135 
$$\epsilon = \frac{S(d \cdot f)^3}{V} \quad (2)$$

1136 where  $d$  = distance the vessel travels in one oscillation (m);  $f$  = frequency of oscillation (Hz),  
1137  $V$  = volume of fluid ( $\text{m}^3$ ), and  $S$  = surface in contact with fluid (as derived from flask  
1138 geometry;  $\text{m}^2$ ). The resultant  $\epsilon$  value will be indicative of the order of magnitude of  $\epsilon$ , not a  
1139 direct equality due to approximation in turbulent length scales.

1140 Building upon this, Guadayol et al. (2009b) empirically formulated a relationship for  $\epsilon$   
1141 based on direct velocity measurements across different frequencies of oscillation and orbit  
1142 diameter:

1143

1144 
$$\epsilon = 10^{(-5.03 - 1.56\phi + f(1.71 + 1.08\phi)) - 5} \quad (3)$$

1145 where  $\phi$  = orbit diameter (cm). Note that Equation (3) only holds for orbital diameters  
1146 between 1.4 - 3.0 cm and oscillation frequencies between 1.19 - 2.54 Hz.

1147

1148 *Vertical grids*

1149 With regards to turbulence generated by vertically-oscillating grids,  $\varepsilon$  can be estimated  
1150 as a function of grid oscillation frequency, stroke length and cosm dimensions (Peters and  
1151 Marrasé, 2000).

1152

1153 
$$\varepsilon = \left(\frac{1}{T/4}\right) \int_0^{T/4} \frac{0.7 \cdot A_{grid}}{V} u(t)^3 dt \quad (4)$$

1154 where  $T$  = period of one oscillation (s),  $A_{grid}$  = solid area of the grid (m<sup>2</sup>), and  $u(t)$  = vertical  
1155 grid velocity (m/s), as calculated from oscillation frequency and stroke length. The 0.7  
1156 coefficient is the empirically derived drag coefficient of a falling grid (Peters and Marrasé,  
1157 2000). Note that this coefficient will change accordingly with different grid geometries and  
1158 configurations; given the ad hoc nature of many turbulence studies, a prudent course of action  
1159 would be to calculate the drag coefficient for different grid setups.

1160 Guadayol et al. (2009b) have also developed a series of empirical equations to  
1161 describe the  $\varepsilon$  at different locations in a tank with a vertically oscillating grid. Equation (5)  
1162 calculates  $\varepsilon$  at a location outside of the grid motion area:

1163

1164 
$$\varepsilon = 2 \times 10^{-6} \cdot s^{9/2} \cdot M^{3/2} \cdot z^{-4} \cdot f^3 \quad (5)$$

1165 where  $s$  = stroke length (cm),  $M$  = mesh size (cm), and  $z$  = distance from the centre of the  
1166 oscillation (cm). Equation (5) holds for stroke lengths between 2.8 - 40 cm; mesh sizes from  
1167 0.9 - 10 cm; and, z-distances between 1 - 73 cm. See Guadayol et al. (2009b) for additional

1168 equations describing  $\varepsilon$  within the grid path as well as variations for constant and sinusoidal  
1169 grid motion.

1170

1171 *Couette cylinders*

1172 In Couette cylinders, the rotational rate and shears can be easily converted to  $\varepsilon$

1173 (Thomas and Gibson, 1990b):

1174

1175 
$$\varepsilon = \nu \left( \frac{R \cdot D \cdot \pi}{60 \cdot G} \right)^2 \quad (6)$$

1176

1177 where  $\nu$  = kinematic viscosity ( $\text{m}^2/\text{s}$ ),  $R$  = rotational rate in revolutions per minute (rpm),  $D$  =

1178 the diameter of the outer cylinder (m), and  $G$  = the gap width (m). Note that the contents of

1179 the parentheses ( $RD\pi/60G$ ) correspond to the value for strain ( $\gamma$ ) in radians per second

1180 (rads/s).

1181

## 1182 **CONCLUSION**

1183 We have observed that experiments involving phytoplankton-turbulence interactions

1184 take many forms often dictated by budget, access to facilities and/or the background

1185 experience of the researchers themselves. This paper aimed to review the various techniques

1186 used to both generate turbulence and quantify the turbulence produced.

1187 With regards to the method of turbulence generation, most (31%) previous cosm work

1188 has been carried out using oscillating grids (as compared to aeration, Couette cylinders and

1189 shaker tables); it is our recommendation that future studies continue to make use of this

1190 method due to operational advantages and a robust set of literature and historical data for

1191 results comparison. Oscillating grids are simple, effective, and inexpensive, with 29 out of 32

1192 studies reviewed quantifying the turbulence produced. The grids themselves can generate  
1193 near-isotropic turbulence across a wide range of scales. A grid setup is relatively low-cost to  
1194 implement or retrofit to existing facilities using basic variable-speed motors. Furthermore,  
1195 grid setups can easily be applied to large tanks ( $>1\text{m}^3$ ) to enable capturing a wider range of  
1196 turbulence length scales. It is important that a mesh barrier (e.g., MacKenzie and Kiørboe  
1197 (1995) be placed between the grid area and the organism to not only reduce the risk of  
1198 mechanical damage but also to create a refuge region that allows the organisms respite from  
1199 the turbulence. Similarly, it is important the grids are programmed accordingly to oscillate at  
1200 a frequency that provides further temporal respite from maximum turbulence. Similarly, the  
1201 cosm itself and the stroke-length over which the grid should oscillate should be on the order  
1202 of at least one metre to properly reflect the natural length scales of vertical overturns.

1203         With regards to our recommendation for quantification methods, Acoustic Doppler  
1204 velocimeters (ADV) are both the most commonly used as well as the least complex and  
1205 inexpensive of the methodologies. However, we do recognise that using an ADV within an  
1206 environment with an oscillating grid does provide some logistical challenges to overcome.

1207         Phytoplankton-turbulence interactions are complex (Figure 1); however, studies of this  
1208 nature are a critical tool for helping us to better understand not only how the aquatic  
1209 environment functions but also how it will respond as climate change continues to alter  
1210 turbulent regimes across the planet (Hallegraeff, 2010; Hinder et al., 2012). Worryingly, the  
1211 number of publications of this nature has been declining in recent years (Figure 6). Only by 1)  
1212 standardising future phytoplankton-turbulence experiments and 2) promoting more  
1213 interdisciplinary collaboration between fluid dynamicists and aquatic ecologists will we be  
1214 able to better understand the subtle, yet dominant and complex, ways that turbulence  
1215 influences the microscopic lives of phytoplankton.



## REFERENCES

- Aguilera, J., C. Jiménez, J. M. Rodríguez-Maroto & F. X. Niell, 1994. Influence of subsidiary energy on growth of *Dunaliella viridis* Teodoresco: the role of extra energy in algal growth. *Journal of Applied Phycology* 6(3):323-330.
- Alcaraz, M., E. Saiz, C. Marrasé & D. Vaqué, 1988. Effects of turbulence on the development of phytoplankton biomass and copepod populations in marine microcosms. *Marine Ecology Progress Series* 49:117 - 125.
- Alexander, A. C., E. Luiker, M. Finley & J. M. Culp, 2016. Chapter 8 - Mesocosm and Field Toxicity Testing in the Marine Context. In Blasco, J., P. M. Chapman, O. Campana & M. Hampel (eds) *Marine Ecotoxicology*. Academic Press, 239-256.
- Allredge, A. L., T. C. Granata, C. C. Gotschalk & T. D. Dickey, 1990. The physical strength of marine snow and its implications for particle disaggregation in the ocean. *Limnology and Oceanography* 35(7):1415-1428.
- Arin, L., C. Marrasé, M. Maar, F. Peters, M. M. Sala & M. Alcaraz, 2002. Combined effects of nutrients and small-scale turbulence in a microcosm experiment. I. Dynamics and size distribution of osmotrophic plankton. *Aquatic Microbial Ecology* 29(1):51-61.
- Bakus, G., J., 1973. Some effects of turbulence and light on competition between two species of phytoplankton. *Investigación Pesquera* 37:87-100.
- Båmstedt, U. & H. Larsson, 2018. An indoor pelagic mesocosm facility to simulate multiple water-column characteristics. *International Aquatic Research* 10(1):13-29.
- Banse, K., 1991. Rates of phytoplankton cell division in the field and in iron enrichment experiments. *Limnology and Oceanography* 36(8):1886-1898.

- Beauvais, S., M. L. Pedrotti, J. Egge, K. Iversen & C. Marrasé, 2006. Effects of turbulence on TEP dynamics under contrasting nutrient conditions: Implications for aggregation and sedimentation processes. *Marine Ecology Progress Series* 323:47-57.
- Behm, J. E., B. R. Waite, S. T. Hsieh & M. R. Helmus, 2018. Benefits and limitations of three-dimensional printing technology for ecological research. *BioMed Central Ecology* 18(1):32-32.
- Berdalet, E., 1992. Effects of turbulence on the marine dinoflagellate *Gymnodinium nelsonii*. *Journal of Phycology* 28(3):267-272.
- Berdalet, E. & M. Estrada, 1993. Effects of turbulence on several phytoplankton species. In Smayda, T. J. & Y. Shimizu (eds) *Toxic Phytoplankton Blooms in the Sea. Developments in Marine Biology*, vol 3. Elsevier, Amsterdam, The Netherlands, 737 - 740.
- Berdalet, E., F. Peters, V. L. Koumandou, C. Roldán, Ò. Guadayol & M. Estrada, 2007. Species-specific physiological response of dinoflagellates to quantified small-scale turbulence. *Journal of Phycology* 43(5):965-977.
- Bergkvist, J., I. Klawonn, M. J. Whitehouse, G. Lavik, V. Brüchert & H. Ploug, 2018. Turbulence simultaneously stimulates small- and large-scale CO<sub>2</sub> sequestration by chain-forming diatoms in the sea. *Nature Communications* 9(1).
- Bienfang, P. K., P. J. Harrison & L. M. Quarmby, 1982. Sinking rate response to depletion of nitrate, phosphate and silicate in four marine diatoms. *Marine Biology* 67(3):295-302.
- Bluteau, C. E., N. L. Jones & G. N. Ivey, 2011. Estimating turbulent kinetic energy dissipation using the inertial subrange method in environmental flows. *Limnology and Oceanography: Methods* 9(7):302-321.
- Chen, D., K. Muda, K. Jones, J. Leftly & P. Stansby, 1998. Effect of shear on growth and motility of *Alexandrium minutum* Halim, a red-tide dinoflagellate. In Reguera, B., J. Blanco, M. L. Fernández & T. Wyatt (eds) *Harmful algae. Xunta de Galicia and Intergovernmental Oceanographic Commission of UNESCO, Vigo, Galicia, Spain*, 352-355.

- Coble, P. G., 2007. Marine Optical Biogeochemistry: The Chemistry of Ocean Color. *Chemical Reviews* 107(2):402-418.
- Couette, M., 1890. Distinction de deux régimes dans le mouvement des fluides. *Journal de Physique Théorique et Appliquée* 9(1):414-424.
- Cózar, A. & F. Echevarría, 2005. Size structure of the planktonic community in microcosms with different levels of turbulence. *Scientia Marina* 69(2):187-197.
- Crimaldi, J. P., 2008. Planar laser induced fluorescence in aqueous flows. *Experiments in Fluids* 44(6):851-863.
- Crossland, N. O. & T. W. La Point, 1992. The design of mesocosm experiments. *Environmental Toxicology and Chemistry* 11(1):1-4.
- Davis, E. A., J. Dedrick, C. S. French, H. W. Milner, J. Myers, J. H. C. Smith & H. A. Spoehr, 1953. Laboratory experiments on *Chlorella* culture at the Carnegie Institution of Washington department of plant biology. In Burlew, J. S. (ed) *Algal Culture from Laboratory to Pilot Plant*. 5th edn. Carnegie Institution of Washington, Washington DC, 105-153.
- Dawidowicz, P., 1990. The effect of *Daphnia* on filament length of blue-green algae. *Hydrobiologia* 191(1):265-268.
- Delaney, M. P., 2003. Effects of temperature and turbulence on the predator-prey interactions between a heterotrophic flagellate and a marine bacterium. *Microbial ecology* 45(3):218-225.
- Dempsey, H. P., 1982. The effects of turbulence on three algae: *Skeletonema costatum*, *Gonyaulax tamarensis*, *Heterocapsa triquetra*. Massachusetts Institute of Technology.
- Dolan, J. R., N. Sall, A. Metcalfe & B. Gasser, 2003. Effects of turbulence on the feeding and growth of a marine oligotrich ciliate. *Aquatic Microbial Ecology* 31(2):183-192.

- Donaghay, P. L. & E. Klos, 1985. Physical, chemical and biological responses to simulated wind and tidal mixing in experimental marine ecosystems. *Marine Ecology Progress Series* 26(1/2):35-45.
- Eder, A., B. Durst & M. Jordan, 2001. Laser-Doppler Velocimetry — Principle and Application to Turbulence Measurements. In Mayinger, F. & O. Feldmann (eds) *Optical Measurements: Techniques and Applications*. Springer, Berlin, Heidelberg, 117-138.
- Eppley, R. W., P. Koeller & G. T. Wallace, 1978. Stirring influences the phytoplankton species composition within enclosed columns of coastal sea water. *Journal of Experimental Marine Biology and Ecology* 32(3):219-239.
- Escaravage, V., L. P. M. J. Wetsteyn, T. C. Prins, A. J. Pouwer, A. de Kruyff, M. Vink-Lievaart, C. M. van der Voom, J. C. H. Peeters & A. C. Smaal, 1997. The impact of marine eutrophication on phytoplankton, zooplankton and benthic suspension feeders. Stratification in mesocosms, a pilot experiment. Ministerie van Verkeer en Waterstaat, The Netherlands, 52.
- Estrada, M., M. Alcaraz & C. Marrasé, 1987. Effects of turbulence on the composition of phytoplankton assemblages in marine microcosms. *Marine Ecology Progress Series* 38:267-281.
- Fogg, G. E. & Than-Tun, 1960. Interrelations of photosynthesis and assimilation of elementary nitrogen in a blue-green alga. *Proceedings of the Royal Society of London Series B Biological Sciences* 153(950):111-127.
- Fraisse, S., M. Bormans & Y. Lagadeuc, 2015. Turbulence effects on phytoplankton morphofunctional traits selection. *Limnology and Oceanography* 60(3):872-884.
- Franks, P. J. S., 2001. Turbulence avoidance: An alternate explanation of turbulence-enhanced ingestion rates in the field. *Limnology and Oceanography* 46(4):959-963.
- Franks, P. J. S. & J. S. Jaffe, 2008. Microscale variability in the distributions of large fluorescent particles observed in situ with a planar laser imaging fluorometer. *Journal of Marine Systems* 69(3):254-270.

- Fuchs, H. L. & G. P. Gerbi, 2016. Seascape-level variation in turbulence- and wave-generated hydrodynamic signals experienced by plankton. *Progress in Oceanography* 141:109-129.
- Garrison, H. S. & K. W. Tang, 2014. Effects of episodic turbulence on diatom mortality and physiology, with a protocol for the use of Evans Blue stain for live–dead determinations. *Hydrobiologia* 738(1):155-170.
- Gibson, C. H. & W. H. Thomas, 1995. Effects of turbulence intermittency on growth inhibition of a red tide dinoflagellate, *Gonyaulax polyedra* Stein. *Journal of Geophysical Research: Oceans* 100(C12):24841-24846.
- Gonzalez-Fernandez, C., J. Toullec, C. Lambert, N. Le Goic, M. Seoane, B. Moriceau, A. Huvet, M. Berchel, D. Vincent, L. Courcot, P. Soudant & I. Paul-Pont, 2019. Do transparent exopolymeric particles (TEP) affect the toxicity of nanoplastics on *Chaetoceros neogracile*? *Environmental Pollution* 250:873-882.
- Grobbelaar, J. U., 1989. Do light/dark cycles of medium frequency enhance phytoplankton productivity? *Journal of Applied Phycology* 1(4):333-340.
- Guadayol, O., C. Marrasé, F. Peters, E. Berdalet, N. Roldá & A. Sabata, 2009a. Responses of coastal osmotrophic planktonic communities to simulated events of turbulence and nutrient load throughout a year. *Journal of Plankton Research* 31(6):583-600.
- Guadayol, Ò., F. Peters, J. E. Stiansen, C. Marrasé & A. Lohrmann, 2009b. Evaluation of oscillating grids and orbital shakers as means to generate isotropic and homogeneous small-scale turbulence in laboratory enclosures commonly used in plankton studies. *Limnology and Oceanography: Methods* 7(APR.):287-303.
- Guasto, J. S., R. Rusconi & R. Stocker, 2012. Fluid mechanics of planktonic microorganisms. *Annual Review of Fluid Mechanics* 44:373 - 400.
- Hallegraeff, G. M., 2010. Ocean climate change, phytoplankton community responses, and harmful algal blooms: a formidable predictive challenge. *Journal of Phycology* 46(2):220-235.

- Havskum, H., 2003. Effects of small-scale turbulence on interactions between the heterotrophic dinoflagellate *Oxyrrhis marina* and its prey, *Isochrysis* sp. *Ophelia* 57(3):125-135.
- Havskum, H. & P. J. Hansen, 2006. Net growth of the bloom-forming dinoflagellate *Heterocapsa triquetra* and pH: Why turbulence matters. *Aquatic Microbial Ecology* 42(1):55-62.
- Havskum, H., P. J. Hansen & E. Berdalet, 2005. Effect of turbulence on sedimentation and net population growth of the dinoflagellate *Ceratium tripos* and interactions with its predator, *Fragilidium subglobosum*. *Limnology and Oceanography* 50(5):1543-1551.
- Hellung-Larsen, P. & I. Lyhne, 1992. Effect of shaking on the growth of diluted cultures of *Tetrahymena*. *The Journal of Protozoology* 39(2):345-349.
- Hinder, S. L., G. C. Hays, M. Edwards, E. C. Roberts, A. W. Walne & M. B. Gravenor, 2012. Changes in marine dinoflagellate and diatom abundance under climate change. *Nature Climate Change* 2(4):271-275.
- Hondzo, M. M., A. Kapur & C. A. Lembi, 1997. The effect of small-scale fluid motion on the green alga *Scenedesmus quadricauda*. *Hydrobiologia* 364(2):225-235.
- Howarth, R. W., T. Butler, K. Lunde, D. Swaney & C. R. Chu, 1993. Turbulence and planktonic nitrogen fixation: a mesocosm experiment. *Limnology and Oceanography* 38(8):1696-1711.
- Hoyer, K., M. Holzner, B. Lüthi, M. Guala, A. Liberzon & W. Kinzelbach, 2005. 3D scanning particle tracking velocimetry. *Experiments in Fluids* 39(5):923.
- Huisman, J., P. Van Oostveen & F. J. Weissing, 1999. Critical depth and critical turbulence: Two different mechanisms for the development of phytoplankton blooms. *Limnology and Oceanography* 44(7):1781-1787.
- Iversen, K. R., R. Primicerio, A. Larsen, J. K. Egge, F. Peters, Ó. Guadayol, A. Jacobsen, H. Havskum & C. Marrasé, 2009. Effects of small-scale turbulence on lower trophic levels under different nutrient conditions. *Journal of Plankton Research* 32(2):197-208.

- Juhl, A. R. & M. I. Latz, 2002. Mechanisms of fluid shear-induced inhibition of population growth in a red-tide dinoflagellate. *Journal of Phycology* 38(4):683-694.
- Juhl, A. R., V. L. Trainer & M. I. Latz, 2001. Effect of fluid shear and irradiance on population growth and cellular toxin content of the dinoflagellate *Alexandrium fundyense*. *Limnology and Oceanography* 46(4):758-764.
- Juhl, A. R., V. Velazquez & M. I. Latz, 2000. Effect of growth conditions on flow-induced inhibition of population growth of a red-tide dinoflagellate. *Limnology and Oceanography* 45(4):905-915.
- Kaku, V. J., M. C. Boufadel & A. D. Venosa, 2006. Evaluation of mixing energy in laboratory flasks used for dispersant effectiveness testing. *Journal of Environmental Engineering* 132(1):93-101.
- Kangas, P. C. & W. H. Adey, 2008. Mesocosm Management. In Jørgensen, S. E. & B. D. Fath (eds) *Encyclopedia of Ecology*. Academic Press, Oxford, 2308-2313.
- Karp-Boss, L., E. Boss & P. A. Jumars, 2000. Motion of dinoflagellates in a simple shear flow. *Limnology and Oceanography* 45(7):1594-1602.
- Karp-Boss, L. & P. A. Jumars, 1998. Motion of diatom chains in steady shear flow. *Limnology and Oceanography* 43(8):1767-1773.
- Katija, K., 2012. Biogenic inputs to ocean mixing. *The Journal of Experimental Biology* 215(6):1040-1049.
- Kilham, P., 1971. A hypothesis concerning silica and the freshwater planktonic diatoms. *Limnology and Oceanography* 16(1):10-18.
- Kjørboe, T., 1993. Turbulence, phytoplankton cell size, and the structure of pelagic food webs. *Advances in Marine Biology* 29:1-72.
- Kjørboe, T., K. P. Andersen & H. G. Dam, 1990. Coagulation efficiency and aggregate formation in marine phytoplankton. *Marine Biology* 107(2):235-245.
- Kirke, B. K., Pumping downwards to prevent algal blooms. In: IWA 2nd World Water Congress, Berlin, 2001.

- Köhler, J., 1997. Measurement of in situ growth rates of phytoplankton under conditions of simulated turbulence. *Journal of Plankton Research* 19(7):849-862.
- Kromkamp, J., F. Schanz, M. Rijkeboer, E. Berdalet, B. Kim & H. J. Gons, 1992. Influence of the mixing regime on algal photosynthetic performance in laboratory scale enclosures. *Hydrobiologia* 238(1):111-118.
- Latz, M. I., J. Allen, S. Sarkar & J. Rohr, 2009. Effect of fully characterized unsteady flow on population growth of the dinoflagellate *Lingulodinium polyedrum*. *Limnology and Oceanography* 54(4):1243-1256.
- Latz, M. I., J. F. Case & R. L. Gran, 1994. Excitation of bioluminescence by laminar fluid shear associated with simple Couette flow. *Limnology and Oceanography* 39(6):1424-1439.
- Latz, M. I., J. C. Nauen & J. Rohr, 2004. Bioluminescence response of four species of dinoflagellates to fully developed pipe flow. *Journal of Plankton Research* 26(12):1529-1546.
- Latz, M. I. & J. Rohr, 1999. Luminescent response of the red tide dinoflagellate *Lingulodinium polyedrum* to laminar and turbulent flow. *Limnology and Oceanography* 44(6):1423-1435.
- Laws, E. A., K. L. Terry, J. Wickman & M. S. Chalup, 1983. A simple algal production system designed to utilize the flashing light effect. *Biotechnology and Bioengineering* 25(10):2319-2335.
- Lazier, J. R. N. & K. H. Mann, 1989. Turbulence and the diffusive layers around small organisms. *Deep Sea Research Part A Oceanographic Research Papers* 36(11):1721-1733.
- Leeuw, T., E. S. Boss & D. L. Wright, 2013. In situ measurements of phytoplankton fluorescence using low cost electronics. *Sensors* 13(6):7872-7883.
- Leterme, S. C., I. Kesaulya, J. G. Mitchell & L. Seuront, 2008. The impact of turbulence and phytoplankton dynamics on foam formation, seawater viscosity and chlorophyll concentrations in the eastern English Channel. *Oceanologia* 50(2):167-182.



- Linares, M. C., 2015. Effects of turbulence and laser exposure on phytoplankton behavior. Universitat Politècnica de Catalunya.
- Liu, F., L. Zeng, Y. H. Wu, B. Baoligao & X. Chen, 2017. Vertical distribution of motile phytoplankton in density currents. In: Li, P. (ed) 3rd International Conference on Water Resource and Environment (WRE 2017), Qingdao, China, 26–29 June 2017. IOP Conference Series: Earth and Environmental Science, vol 82. IOP Publishing, p 012073.
- Llaveria, G., E. Garcés, O. N. Ross, R. I. Figueroa, N. Sampedro & E. Berdalet, 2010. Small-scale turbulence can reduce parasite infectivity to dinoflagellates. *Marine Ecology Progress Series* 412:45-56.
- Lohrmann, A., R. Cabrera, G. Gelfenbaum & J. Haines, 1995. Direct measurements of Reynolds stress with an acoustic Doppler velocimeter. In: Anderson, S.P., G.F. Appell & A. J. Williams III (eds) Proceedings of the IEEE Fifth Working Conference on Current Measurement, St. Petersburg, FL, USA, 7-9 Feb 1995. IEEE, p 205-210.
- Long, J. D., G. W. Smalley, T. Barsby, J. T. Anderson & M. E. Hay, 2007. Chemical cues induce consumer-specific defenses in a bloom-forming marine phytoplankton. *Proceedings of the National Academy of Sciences* 104(25):10512-10517.
- Lüring, M., 1998. Effect of grazing-associated infochemicals on growth and morphological development in *Scenedesmus acutus* (Chlorophyceae). *Journal of Phycology* 34(4):578-586.
- Maar, M., L. Arin, R. Simó, M.-M. Sala, F. Peters & C. Marrasé, 2002. Combined effects of nutrients and small-scale turbulence in a microcosm experiment. II. Dynamics of organic matter and phosphorus. *Aquatic Microbial Ecology* 29(1):63-72.
- MacKenzie, B. R. & T. Kiørboe, 1995. Encounter rates and swimming behavior of pause-travel and cruise larval fish predators in calm and turbulent laboratory environments. *Limnology and Oceanography* 40(7):1278-1289.

- Margalef, R., 1997. Turbulence and marine life. In: Marrasé, C., E. Saiz & J. M. Redondo (eds) *Scientia Marina: Lectures on plankton and turbulence*. Vol 61 (SUPPL.1), 109-123.
- Marrasé, C., J. H. Costello, T. Granata & J. R. Strickler, 1990. Grazing in a turbulent environment: Energy dissipation, encounter rates, and efficacy of feeding currents in *Centropages hamatus*. *Proceedings of the National Academy of Sciences of the United States of America* 87(5):1653-1657.
- Martin, J. H. & R. Michael Gordon, 1988. Northeast Pacific iron distributions in relation to phytoplankton productivity. *Deep Sea Research Part A Oceanographic Research Papers* 35(2):177-196.
- Martínez, R. A., A. Calbet & E. Saiz, 2017. Effects of small-scale turbulence on growth and grazing of marine microzooplankton. *Aquatic Sciences* 80(1).
- Matheson, F. E., 2008. Microcosms. In Jørgensen, S. E. & B. D. Fath (eds) *Encyclopedia of Ecology*. Academic Press, Oxford, 2393-2397.
- Metcalf, A. M., T. J. Pedley & T. F. Thingstad, 2004. Incorporating turbulence into a plankton foodweb model. *Journal of Marine Systems* 49(1-4):105-122.
- Moisander, P. H., J. L. Hench, K. Kononen & H. W. Paerl, 2002. Small-scale shear effects on heterocystous cyanobacteria. *Limnology and Oceanography* 47(1):108-119.
- Musielak, M. M., L. E. E. Karp-Boss, P. A. Jumars & L. J. Fauci, 2009. Nutrient transport and acquisition by diatom chains in a moving fluid. *Journal of Fluid Mechanics* 638:401-421.
- Naselli-Flores, L., T. Zohary & J. Padisák, 2020. Life in suspension and its impact on phytoplankton morphology: an homage to Colin S. Reynolds. *Hydrobiologia* 848:7-30 (2021).
- Nedbal, L., V. Tichý, F. Xiong & J. U. Grobbelaar, 1996. Microscopic green algae and cyanobacteria in high-frequency intermittent light. *Journal of Applied Phycology* 8(4):325-333.

- Nejstgaard, J., C. , L.-J. Naustvoll & A. Sazhin, 2001a. Correcting for underestimation of microzooplankton grazing in bottle incubation experiments with mesozooplankton. *Marine Ecology Progress Series* 221:59-75.
- Nejstgaard, J., C., B. H. Hygum, L.-J. Naustvoll & U. Båmstedt, 2001b. Zooplankton growth, diet and reproductive success compared in simultaneous diatom- and flagellate-microzooplankton-dominated plankton blooms. *Marine Ecology Progress Series* 221:77-91.
- Nerheim, S., J. E. Stiansen & H. Svendsen, 2002. Grid-generated turbulence in a mesocosm experiment. *Hydrobiologia* 484:61-73.
- Odum, E. P., 1984. The Mesocosm. *BioScience* 34(9):558-562.
- Okubo, A., 1976. Remarks on the use of 'diffusion diagrams' in modeling scale-dependent diffusion. *Deep Sea Research and Oceanographic Abstracts* 23(12):1213-1214.
- Oviatt, C. A., 1981. Effects of different mixing schedules on phytoplankton, zooplankton and nutrients in marine microcosms. *Marine Ecology Progress Series* 4:57-67.
- Paczkowska, J., O. F. Rowe, L. Schlüter, C. Legrand, B. Karlson & A. Andersson, 2017. Allochthonous matter: An important factor shaping the phytoplankton community in the Baltic Sea. *Journal of Plankton Research* 39(1):23-34.
- Padisák, J., É. Soróczki-Pintér & Z. Reznér, 2003. Sinking properties of some phytoplankton shapes and the relation of form resistance to morphological diversity of plankton - an experimental study. *Hydrobiologia* 500:243-257.
- Pahlow, M., U. Riebesell & D. A. Wolf-Gladrow, 1997. Impact of cell shape and chain formation on nutrient acquisition by marine diatoms. *Limnology and Oceanography* 42(8):1660-1672.

- Pannard, A., M. Bormans, S. Lefebvre, P. Claquin & Y. Lagadeuc, 2007. Phytoplankton size distribution and community structure: influence of nutrient input and sedimentary loss. *Journal of Plankton Research* 29(7):583-598.
- Parsons, T. R., P. J. Harrison & R. Waters, 1978. An experimental simulation of changes in diatom and flagellate blooms. *Journal of Experimental Marine Biology and Ecology* 32(3):285-294.
- Pasciak, W. J. & J. Gavis, 1975. Transport limited nutrient uptake rates in *Ditylum brightwellii*. *Limnology and Oceanography* 20(4):604-617.
- Peters, F., L. Arin, C. Marrasé, E. Berdalet & M. M. Sala, 2006. Effects of small-scale turbulence on the growth of two diatoms of different size in a phosphorus-limited medium. In: Peters, F. & C. Hannah (eds) *Workshop on Future Directions in Modelling Physical-Biological Interactions (WKFDPI)*, Barcelona, Catalunya, Spain, 7-9 March 2004. *Journal of Marine Systems* 61(3-4):134-148.
- Peters, F., J. W. Choi & T. Gross, 1996. *Paraphysomonas imperforata* (Protista, Chrysomonadida) under different turbulence levels: feeding, physiology and energetics. *Marine Ecology Progress Series* 134:235-245.
- Peters, F. & T. Gross, 1994. Increased grazing rates of microplankton in response to small-scale turbulence. *Marine Ecology Progress Series* 115(3):299-308.
- Peters, F. & C. Marrasé, 2000. Effects of turbulence on plankton: An overview of experimental evidence and some theoretical considerations. *Marine Ecology Progress Series* 205:291-306.
- Peters, F., C. Marrasé, H. Havskum, F. Rassoulzadegan, J. Dolan, M. Alcaraz & J. M. Gasol, 2002. Turbulence and the microbial food web: Effects on bacterial losses to predation and on community structure. *Journal of Plankton Research* 24(4):321-331.
- Peters, F. & J. M. Redondo, 1997. Turbulence generation and measurement: Application to studies on plankton. In: Marrasé, C., E. Saiz & J. M. Redondo (eds) *Scientia Marina: Lectures on plankton and turbulence*. Vol 61 (SUPPL.1), 205-228.

- Petersen, J. E., L. P. Sanford & W. M. Kemp, 1998. Coastal plankton responses to turbulent mixing in experimental ecosystems. *Marine Ecology Progress Series* 171:23-41.
- Pollingher, U. & E. Zemel, 1981. In situ and experimental evidence of the influence of turbulence on cell division processes of *Peridinium cinctum* forma *westii* (Lemm.) Lefèvre. *British Phycological Journal* 16(3):281-287.
- Prairie, J. C., K. R. Sutherland, K. J. Nickols & A. M. Kaltenberg, 2012. Biophysical interactions in the plankton: A cross-scale review. *Limnology and Oceanography: Fluids and Environments* 2(1):121-145.
- Pringle, J. M., 2007. Turbulence avoidance and the wind-driven transport of plankton in the surface Ekman layer. *Continental Shelf Research* 27(5):670-678.
- Raffel, M., C. E. Willert, F. Scarano, C. J. Kähler, S. T. Wereley & J. Kompenhans, 2018. Particle image velocimetry: a practical guide. Springer.
- Regel, R. H., J. D. Brookes, G. G. Ganf & R. W. Griffiths, 2004. The influence of experimentally generated turbulence on the Mash01 unicellular *Microcystis aeruginosa* strain. *Hydrobiologia* 517(1):107-120.
- Reynolds, C. S., 2009. Biological–Physical Interactions. In Likens, G. E. (ed) *Encyclopedia of Inland Waters*. Academic Press, Oxford, 515-521.
- Richmond, A. & A. Vonshak, 1978. Spirulina culture in Israel. *Archiv für Hydrobiologie - Beihefte Ergebnisse der Limnologie* 11:274 - 280.
- Rijkeboer, M., F. de Bles & H. J. Gons, 1990. Laboratory scale enclosure: concept, construction and operation. *Journal of Plankton Research* 12(1):231-244.
- Rohr, J., J. Allen, J. Losee & M. I. Latz, 1997. The use of bioluminescence as a flow diagnostic. *Physics Letters A* 228(6):408-416.

- Rohr, J., M. Hyman, S. Fallon & M. I. Latz, 2002. Bioluminescence flow visualization in the ocean: an initial strategy based on laboratory experiments. *Deep Sea Research Part I: Oceanographic Research Papers* 49(11):2009-2033.
- Rohr, J., J. Losee & J. Hoyt, 1990. Stimulation of bioluminescence by turbulent pipe flow. *Deep Sea Research Part A, Oceanographic Research Papers* 37(10):1639-1646.
- Ross, O. N. & J. Sharples, 2007. Phytoplankton motility and the competition for nutrients in the thermocline. *Marine Ecology Progress Series* 347:21-38.
- Ross, O. N. & J. Sharples, 2008. Swimming for survival : A role of phytoplankton motility in a stratified turbulent environment. *Journal of Marine Systems* 70(3-4):248-262.
- Rothschild, B. J. & T. R. Osborn, 1988. Small-scale turbulence and plankton contact rates. *Journal of Plankton Research* 10(3):465-474.
- Saiz, E. & M. Alcaraz, 1992. Free-swimming behaviour of *Acartia clausi* (Copepoda: Calanoida) under turbulent water movement. *Marine Ecology Progress Series* 80(2-3):229-236.
- Saiz, E. & T. Kiørboe, 1995. Predatory and suspension feeding of the copepod *Acartia tonsa* in turbulent environments. *Oceanographic Literature Review* 43(1):59.
- Sanford, L. P., 1997. Turbulent mixing in experimental ecosystem studies. *Marine Ecology Progress Series* 161:265-293.
- Santschi, P. H., 1985. The MERL mesocosm approach for studying sediment-water interactions and ecotoxicology. *Environmental Technology Letters* 6(1-11):335-350.
- Sato, T., D. Yamada & S. Hirabayashi, 2010. Development of virtual photobioreactor for microalgae culture considering turbulent flow and flashing light effect. *Energy Conversion and Management* 51(6):1196-1201.

- Savidge, G., 1981. Studies of the effects of small-scale turbulence on phytoplankton. *Journal of the Marine Biological Association of the United Kingdom* 61(2):477-488.
- Scarano, F., 2012. Tomographic PIV: principles and practice. *Measurement Science and Technology* 24(1):012001.
- Schapiro, M., L. Seuront & V. Gentilhomme, 2006. Effects of small-scale turbulence on *Phaeocystis globosa* (Prymnesiophyceae) growth and life cycle. *Journal of Experimental Marine Biology and Ecology* 335(1):27-38.
- Schöne, H., 1970. Untersuchungen zur ökologischen Bedeutung des Seegangs für das Plankton mit besonderer Berücksichtigung mariner Kieselalgen. *Internationale Revue der gesamten Hydrobiologie und Hydrographie* 55(4):595-677.
- Schwartz, E. R., R. X. Poulin, N. Mojib & J. Kubanek, 2016. Chemical ecology of marine plankton. *Natural Product Reports* 33(7):843-860.
- Sengupta, A., F. Carrara & R. Stocker, 2017. Phytoplankton can actively diversify their migration strategy in response to turbulent cues. *Nature* 543:555-558.
- Simoncelli, S., S. J. Thackeray & D. J. Wain, 2019. Effect of temperature on zooplankton vertical migration velocity. *Hydrobiologia* 829(1):143-166.
- Smayda, T. J. & C. S. Reynolds, 2001. Community assembly in marine phytoplankton: Application of recent models to harmful dinoflagellate blooms. *Journal of Plankton Research* 23(5):447-461.
- Smith, B. C. & A. Persson, 2005. Synchronization of encystment of *Scrippsiella lachrymosa* (Dinophyta). *Journal of Applied Phycology* 17(4):317-321.
- Solomon, K. R. & M. Hanson, 2014. Mesocosms and Microcosms (Aquatic) *Encyclopedia of Toxicology: Third Edition*. 223-226.

- Sonntag, N. C. & T. R. Parsons, 1979. Mixing an enclosed, 1300m<sup>3</sup> water column: effects on the planktonic food web. *Journal of Plankton Research* 1(1):85-102.
- Staehr, P. A. & K. Sand-Jensen, 2006. Seasonal changes in temperature and nutrient control of photosynthesis, respiration and growth of natural phytoplankton communities. *Freshwater Biology* 51(2):249-262.
- Steele, J. H., D. M. Farmer & E. W. Henderson, 1977. Circulation and temperature structure in large marine enclosures. *Journal of the Fisheries Research Board of Canada* 34(8):1095-1104.
- Stoecker, D. K., A. Long, S. E. Suttles & L. P. Sanford, 2006. Effect of small-scale shear on grazing and growth of the dinoflagellate *Pfiesteria piscicida*. *Harmful Algae* 5(4):407-418.
- Stokes, M. D., G. B. Deane, M. I. Latz & J. Rohr, 2004. Bioluminescence imaging of wave-induced turbulence. *Journal of Geophysical Research: Oceans* 109(C1):1-8.
- Striebel, M., L. Kirchmaier & P. Hingsamer, 2013. Different mixing techniques in experimental mesocosms—does mixing affect plankton biomass and community composition? *Limnology and Oceanography: Methods* 11(4):176-186.
- Sullivan, J. M. & E. Swift, 2003. The effect of small-scale turbulence on net growth rate and size of ten species of marine dinoflagellates. *Journal of Phycology* 39:83-94.
- Sullivan, J. M., E. Swift, P. L. Donaghay & J. E. B. Rines, 2003. Small-scale turbulence affects the division rate and morphology of two red-tide dinoflagellates. *Harmful Algae* 2(3):183-199.
- Svensen, C., J. K. Egge & J. E. Stiansen, 2001. Can silicate and turbulence regulate the vertical flux of biogenic matter? A mesocosm study. *Marine Ecology Progress Series* 217:67-80.
- Sverdrup, H. U., 1953. On conditions for the vernal blooming of phytoplankton. *ICES Journal of Marine Science* 18(3):287-295.



- Talling, J. F., 1960. Comparative laboratory and field studies of photosynthesis by a marine planktonic diatom. *Limnology and Oceanography* 5(1):62-77.
- Thomas, W. H. & C. H. Gibson, 1990a. Effects of small-scale turbulence on microalgae. *Journal of Applied Phycology* 2(1):71-77.
- Thomas, W. H. & C. H. Gibson, 1990b. Quantified small-scale turbulence inhibits a red tide dinoflagellate, *Gonyaulax polyedra* Stein. *Deep Sea Research Part A Oceanographic Research Papers* 37(10):1583-1593.
- Thomas, W. H. & C. H. Gibson, 1992. Effects of quantified small-scale turbulence on the dinoflagellate, *Gymnodium sanguineum (splendens)*: contrasts with *Gonyaulax (Lingulodinium) polyedra*, and the fishery implication. *Deep Sea Research Part A Oceanographic Research Papers* 39(7):1429-1437.
- Thomas, W. H., D. L. R. Seibert, M. Alden, A. Neori & P. Eldridge, 1984a. Yields, photosynthetic efficiencies and proximate composition of dense marine microalgal cultures. I. Introduction and *Phaeodactylum tricornutum* experiments. *Biomass* 5(3):181-209.
- Thomas, W. H., D. L. R. Seibert, M. Alden, A. Neori & P. Eldridge, 1984b. Yields, photosynthetic efficiencies and proximate composition of dense marine microalgal cultures. II. *Dunaliella primolecta* and *Tetraselmis suecica* experiments. *Biomass* 5(3):211-225.
- Thomas, W. H., D. L. R. Seibert, M. Alden, A. Neori & P. Eldridge, 1984c. Yields, photosynthetic efficiencies and proximate composition of dense marine microalgal cultures. III. *Isochrysis* sp. and *Monallantus salina* experiments and comparative conclusions. *Biomass* 5(4):299-316.
- Thomas, W. H., C. T. Tynan & C. H. Gibson, 1997. Turbulence-phytoplankton interrelationships. In Round, F. E. & D. J. Chapman (eds) *Progress in Phycological Research*. vol 12. Biopress Ltd, Bristol, UK, 283-324.
- Tropea, C. & A. L. Yarin, 2007. *Springer handbook of experimental fluid mechanics*. Springer Science & Business Media.

- Turkoglu, M., 2013. Red tides of the dinoflagellate *Noctiluca scintillans* associated with eutrophication in the Sea of Marmara (the Dardanelles, Turkey). *Oceanologia* 55(3):709-732.
- Tuttle, R. C. & A. R. Loeblich, 1975. An optimal growth medium for the dinoflagellate *Cryptothecodinium cohnii*. *Phycologia* 14(1):1-8.
- Tynan, C. T., 1993. The effects of small-scale turbulence on dinoflagellates. University of California, San Diego.
- Visser, P. M., B. W. Ibelings, M. Bormans & J. Huisman, 2016. Artificial mixing to control cyanobacterial blooms: a review. *Aquatic Ecology* 50(3):423-441.
- Waller, W. T. & H. J. Allen, 2008. Acute and Chronic Toxicity. In Jørgensen, S. E. & B. D. Fath (eds) *Encyclopedia of Ecology*. Academic Press, Oxford, 32-43.
- Walsby, A. E., 1971. Pressure relationships of gas vacuoles. *Proceedings of the Royal Society of London B* 178:301-326.
- Warnaars, T. A., M. Hondzo & M. A. Carper, 2006. A desktop apparatus for studying interactions between microorganisms and small-scale fluid motion. *Hydrobiologia* 563(1):431-443.
- Waterhouse, A. F., J. A. MacKinnon, J. D. Nash, M. H. Alford, E. Kunze, H. L. Simmons, K. L. Polzin, L. C. S. Laurent, O. M. Sun, R. Pinkel, L. D. Talley, C. B. Whalen, T. N. Huussen, G. S. Carter, I. Fer, S. Waterman, A. C. N. Garabato, T. B. Sanford & C. M. Lee, 2014. Global patterns of diapycnal mixing from measurements of the turbulent dissipation rate. *Journal of Physical Oceanography* 44(7):1854-1872.
- Webster, D. R., A. Brathwaite & J. Yen, 2004. A novel laboratory apparatus for simulating isotropic oceanic turbulence at low Reynolds number. *Limnology and Oceanography: Methods* 2(JAN.):1-12.
- Webster, D. R., P. J. W. Roberts & L. Ra'ad, 2001. Simultaneous DPTV/PLIF measurements of a turbulent jet. *Experiments in Fluids* 30(1):65-72.

- White, A. W., 1976. Growth inhibition caused by turbulence in the toxic marine dinoflagellate *Gonyaulax excavata*. Journal of the Fisheries Research Board of Canada 33(11):2598-2602.
- Wüest, A. & A. Lorke, 2003. Small-scale hydrodynamics in lakes. Annual Review of fluid mechanics 35(1):373-412.
- Xu, D. & J. Chen, 2013. Accurate estimate of turbulent dissipation rate using PIV data. Experimental Thermal and Fluid Science 44:662-672.
- Yeung, P. K. K. & J. T. Y. Wong, 2003. Inhibition of cell proliferation by mechanical agitation involves transient cell cycle arrest at G1 phase in dinoflagellates. Protoplasma 220(3):173-178.
- Yousif, E. & R. Haddad, 2013. Photodegradation and photostabilization of polymers, especially polystyrene: review. Springerplus 2:398-398.
- Zhou, J., X. Han, B. Qin, C. Casenave & G. Yang, 2016. Response of zooplankton community to turbulence in large, shallow Lake Taihu: a mesocosm experiment. Fundamental and Applied Limnology / Archiv für Hydrobiologie 187(4):325-324.
- Zirbel, M. J., F. Veron & M. I. Latz, 2000. The reversible effect of flow on the morphology of *Ceratocorys horrida* (Peridinales, Dinophyta). Journal of Phycology 36(1):46-58.

## APPENDIX 1 - Lesser-used turbulence-generation techniques

Having covered the main techniques used to generate turbulence in the laboratory, it is also worth discussing more novel or lesser-used techniques, including pumping, magnetic stirrers, rotating chambers, wave tanks, impellers/propellers, paddles, dialysis cylinders, and convective mixing.

*Pumping:* As is common practice in aquaria, water may be introduced via a pump. This manner of turbulence generation is unrepresentative of natural turbulence as mixing would be greatest adjacent to the outflow and would quickly attenuate with distance (Sanford, 1997). Depending on the length of study, the effectiveness of the pumps may become reduced with time due to biofouling clogging pipes and pumps (Kangas and Adey, 2008). Using an array of hydraulic actuator pumps placed at the corners of a cubic tank, Webster et al. (2004) produced near-isotropic homogeneous turbulence comparing the flow characteristics with other studies using grids. The absence of moving structures inside the tank not only facilitates current measurements but also reduced the risk of mechanically damaging the organisms. Subsurface pumps can also be used to simulate surface wind-waves within a tank (Zhou et al., 2016). Laboratory flume tanks also use pump systems to produce specific flow regimes, generating a variety of  $\epsilon$  under both laminar and turbulent regimes. A number of studies were carried out on different bioluminescent dinoflagellates to ascertain the threshold shear required to make them bioluminesce (Rohr et al., 1990; Latz and Rohr, 1999; Latz et al., 2004; Latz et al., 2009). Once this relationship has been determined, this threshold can be used to calculate the turbulence by recording the bioluminescence intensity. By using aerofoils in a flume tank, Laws et al. (1983) promoted turbulence eddies; as water moves at a critical flow velocity over the aerofoils, pressure differentials above and below produce turbulent vortices resulting in a yield doubling of the diatom *Phaeodactylum tricornutum* Bohlin.

*Magnetic stirrers:* Magnetic stirring devices are commonly used to agitate chemical solutions. The resulting turbulence profile produced in a vessel is inverted when compared to those in nature.

Typically, a water column will exhibit a wind- and convection-mixed turbulent upper layer with  $\epsilon$  decreasing with depth. Large flows can cause mixing at depth via bed friction which can result in high levels of turbulence. However, this would need to occur in a water column that is suitably shallow enough to allow this bottom-generated turbulence to propagate up into the photic layer for this to be applicable within a cosm context. In addition, the turbulence field generated from magnetic stirrers is difficult to measure accurately so any biological changes are difficult to attribute to a particular flow characteristic (Warnaars et al., 2006). Researching optimal growth conditions for the dinoflagellate *Cryptocodinium cohnii*, Tuttle and Loeblich (1975) compared cell growth from cultures subjected to rotary shakers and magnetic stirrers before concluding that the shaker intensities used in the experiment damaged cells with no significant increase in growth compared to cultures exposed to magnetic stirring.

*Rotating chambers:* An enclosed chamber can be constructed that rotates in the z-axis. This technique is useful when studying the effects of vertical mixing especially on species that exhibit gravitaxis or have a preferential swimming / buoyancy direction. Sengupta et al. (2017) made use of a space-saving and cost-effective turbulence generation technique via a millimetre-scale “millifluidic chamber”. Attached to a computer-controlled motor, the chamber could be programmed to mimic vertical overturning, specifically designed to be the same order of magnitude as Kolmogorov scale overturns.

*Wave tanks:* As with flume tanks, many laboratories now also have separate wave tanks or the ability to convert an existing flume tank. It can be difficult to directly measure the turbulent field associated with wave events due to surface oscillations and cavitation which interfere with velocity probes that need to be constantly submerged. As such, Stokes et al. (2004) developed a novel technique utilising bioluminescent dinoflagellates to correlate the intensity of light emitted to  $\epsilon$  within a wave. Waves were computer-generated to consistently break at the same location while a

slow-motion digital camera was used to photograph the breaker with pixel light intensity of the image being related to the shear stress the organism was subjected to.

*Impellers/propellers:* A benefit of using propellers to produce turbulence in the laboratory is that the equipment is relatively low-cost and off-the-shelf, coming in a variety of different sizes and materials. Furthermore, the propellers can be easily attached to variable speed motors to produce a range of turbulent intensities. The propeller / impellor can have a profound effect on the circulation within the tank with radial impellers (vertical blades attached to a horizontal disc) resulting in two pairs of convective cells while axial impellers (akin to a boat propeller) cause a single pair of convective cells. The impellers can be sized appropriately and spin at specific speeds to either promote tank circulation or to generate localised turbulence; Sanford (1997) recommends a balance between these two extremes. A propeller system was used by Garrison and Tang (2014) to test the effect of high intensity episodic turbulence on diatoms noting an increase in cell mortality after exposure of only 45 seconds. Impellor like-structures have been used in a number of longer-duration multi-trophic experiments involving natural populations of phytoplankton and zooplankton (Donaghay and Klos, 1985; Escaravage et al., 1997; Petersen et al., 1998). These set-ups involve a central shaft with rods / paddles attached at specific depths to promote vertical stratification with separate well-mixed layers mirroring an upper wind-mixed layer with a lower mixed layer. The rotational direction is alternated to prevent whirlpool mixing that would transfer water from one layer to another. In order to simulate a reduction in flow that would normally be associated with tidal slack, Petersen et al. (1998) stopped the rotational mixing periodically. Donaghay and Klos (1985) used a variety of horizontal paddles at different depths to produce two separate well-mixed layers; a physical regime found in nature that is difficult to replicate using other methods of turbulence generation.

*Paddles:* Mechanised paddles can be placed into a cosm with the size, orientation and placement of the paddles altered at the discretion of the researcher. The paddles can oscillate horizontally or

vertically with the agitation produced increasing with distance from the pivot. As such, it may be prudent to opt for a rotating paddle (analogous to a watermill wheel) to ensure more isotropic conditions (Richmond and Vonshak, 1978; Dempsey, 1982).

*Dialysis cylinders:* Analogous to a small limnocorral, Köhler (1997) placed a natural population of phytoplankton into a 650ml transparent cylinder and suspended it into various aquatic environments. Using a lift system, the cylinder was suspended at depth and oscillated vertically through the water column at various amplitudes, frequencies and durations to mirror natural vertical mixing. The water within the cylinder was homogenised via a single paddle mounted on the inner edge of the cylinder, mixing the internal fluid as the cylinder rolled.

*Convective mixing:* It is possible to generate convective mixing within a cosm by either applying a heat source at the base (causing the water to rise) or by cooling the surface (causing the water to sink). The convective cell(s) established can be described as a function of water depth and the temperature difference between the top and bottom of the tank; high temperatures on the surface reducing to lower temperatures at depth will clearly result in a classic stratified water column with a distinct thermocline. Inverting this set-up by cooling the surface water and gently heating the water depth will result in a constant thermal instability mimicking the advection of water akin to a turbulent overturn. If carried out in suitably sized cosms (of the scale of natural turbulent overturns), this technique generates vertical turbulent overturns that more closely match those found in nature. Thus, the light climate that the planktonic organisms experience would be more realistic with regards to vertical distances moved. Båmstedt and Larsson (2018) showcased the convective-mixing abilities of the cosm facilities at Umeå Marine Science Centre, Sweden. Each 5m-high mesocosm is surrounded by three vertical sections into which flows a solution which can be heated or cooled to produce specific temperature profiles. This can be used to replicate the natural thermoclinic temperature structures, but by inverting the temperature profile via mild heating at

depth, it is possible to cause convective overturning. A larger temperature difference between the top section and the lower section causes a greater degree of convective flow.



## **APPENDIX 2 - Lesser-used techniques for quantifying turbulence**

*Dye dispersion:* Dye tracing involves the release of a fluorescent dye product into a mesocosm in order to approximate turbulent mixing. The dye is released at mid-depths and then monitored by either taking water samples at depth, by pumping water at depth through a surface fluorometer or by conducting fluorimetry profiles with depth. Working on the CEPEX array, Steele et al. (1977) used dye dispersion to quantify vertical diffusivity for a number of mesocosm studies (Eppley et al., 1978; Sonntag and Parsons, 1979). By measuring the vertical distribution of the dye with time, Steele et al. (1977) were able to not only observe the gradual homogenisation of the dye concentration but also observed the development of a secondary patch of dye concentration at depth.

Clearly the dye substance that is used to measure flow should be inert so as to not react with any surfaces / materials within the tank. Furthermore, the substance should not be toxic nor should it act as or decay into a chemical species that could influence growth rate of any phytoplankton / bacteria within the experiment. For example, Båmstedt and Larsson (2018) introduced humic acid as a marker dispersant in their initial mixing studies before switching to rhodamine dye. Humic acid can decompose into other bioactive compounds / nutrients so could influence phytoplankton growth with time. Furthermore, the addition of an acid would alter the gas solubility of the water as well as biasing any biological experiment towards low-pH tolerant species. At high concentrations, rhodamine dye would affect light transmission through the water especially towards the UV end of the spectrum.

*Bioluminescence:* Certain species of dinoflagellates are known to exhibit bioluminescence, producing a brilliant blue light when exposed to species-dependent shear flows. As well as flow regime, dinoflagellate cells have been shown to exhibit bioluminescent tendencies under a variety of rapidly changing factors including thermal, pH, chemical, electrical and osmotic pressure (see

references in Stokes et al. (2004)). While this technique is applicable to flow visualisation in turbulent fields, it is restricted to studies of bioluminescent organisms alone. It is not recommended to add bioluminescent organisms to cosms with other species present as this would bias the population dynamics considerably. Firstly, a number of bioluminescent species are allelopathic, producing toxins that impede motility, growth rates and nutrient uptake rates (Schwartz et al., 2016). Other species, such as *Noctiluca scintillans* (Macartney) Kofoid & Swezy, are carnivorous so would skew population growth measurements via grazing. Furthermore, carnivorous dinoflagellates of this type excrete ammonia which can cause subsequent growth rate changes in different groups (Turkoglu, 2013).

Using colonies of *Pyrocystis fusiformis* C.W.Thomson, Stokes et al. (2004) used a wave tank and an intensified slow-motion camera to record the light emitted by the cells in a breaking wave. Firstly, the cell anxiety parameter for the species is calculated from observations; this factor is an inherent property of the cell which dictates the likelihood that the cell will emit light given a certain environmental perturbation. The pixel intensity is recorded then used to estimate the local shear stress in the fluid medium which can then be converted into shear stress values and  $\epsilon$ . The digital images produced are effectively 2D maps showing the quantitative evolution of a breaking wave with time.

While this technique can be used to quickly produce a spatial map of  $\epsilon$ , it does come with some bias namely the presence of bubbles which scatter / absorb the emitted light. It is possible to omit the effects of bubbles by subtracting the mean intensity recorded in a process known as thresholding. Thresholding itself is a subjective process so it is crucial that the same threshold level is applied to all images. The images can be adjusted so as to remove light occurring outside of the perturbation (e.g. behind the breaking wave) and those that exhibit radically different light properties. It is proposed to use a light source of known intensity placed in the sample region so as to properly account for the scattering / absorption effects of bubbles. Another factor to consider is that of cell

memory; a measure of how the cells may adapt to the conditions they are being exposed to and alter their light emission accordingly (Stokes et al., 2004). As well as wave tanks, flume tanks have also been used in studies where the response of a given bioluminescent species can be monitored with regards to different flow rate shear stresses under both laminar and turbulent regimes (Rohr et al., 1990; Latz and Rohr, 1999).

Depending on the level of  $\varepsilon$  encountered, it is possible to use different bioluminescent species that exhibit different trigger thresholds. In an experiment aiming to observe laminar and turbulent flow in pipes, Latz et al. (2004) experimented with four different dinoflagellate species with the aim of producing a shear sensitivity hierarchy. As well as exhibiting shear thresholds ranging across an order of magnitude, the cells also display a range of morphological differences being fusiform, spherical and spined. As the flow rate in the pipe apparatus was altered in the presence of the different species, light flashes were recorded using a photon-counting photomultiplier system.

**APPENDIX 3 - Summary table of known phytoplankton-turbulence experiments**

<b>Turbulence Method</b>	<b>Cosm material</b>	<b>Approx. cosm volume (m<sup>3</sup>)</b>	<b>Organism(s)</b>	<b>Turbulence Dissipation Rate Range (m<sup>2</sup>/s<sup>3</sup>) (or equivalent parameter)</b>	<b>Reference</b>
Aeration	Glass	2.5 x 10 <sup>-3</sup>	Green algae – <i>Dunaliella viridis</i> Teodoresco	6.8 x 10 <sup>-5</sup> to 4.8 x 10 <sup>-3</sup>	Aguilera et al. (1994)
Aeration	Glass	1.0 x 10 <sup>-3</sup>	Green algae – <i>Scenedesmus obliquus</i> (Turpin) Kützing, <i>Stichococcus</i> sp.	None	Bakus (1973)
Aeration	Unspecified	2.5 x 10 <sup>-2</sup>	Natural population including: Diatoms: <i>Skeletonema costatum</i> (Greville) Cleve, <i>Chaetoceros</i> sp., <i>Lauderia</i> sp., <i>Thalassiosira cf. hyalina</i> (Grunow) Gran, <i>Thalassiosira cf. allenii</i> H.Takano, <i>Pseudonitzschia</i> sp, <i>Guinardia</i> sp.,	10 <sup>-3</sup> to 10 <sup>-1</sup>	Cózar and Echevarría (2005)

Aeration	Polyethylene	6.65 x 10 <sup>1</sup>	<p>Natural population including:</p> <p>Diatoms – <i>Chaetoceros socialis</i> H.S.Lauder, <i>Stephanopyxis palmeriana</i> (Greville) Grunow, <i>Pseudo-nitzschia pungens</i> (Grunow ex Cleve) Hasle <sup>a</sup>, <i>Coscinodiscus wailesii</i> Gran &amp; Angst</p> <p>Dinoflagellates - <i>Dinophysis</i> sp., <i>Amphidinium</i> sp., <i>Peridinium</i> sp., <i>Gymnodinium</i> sp., <i>Noctiluca</i> sp.</p> <p>Ciliates – <i>Eutintinnus pectinis</i> Kofoid &amp; Campbell, <i>Favella ehrenbergii</i> (Claparède &amp; Lachmann) Jörgensen, <i>Helicostomella subulate</i> (Ehrenberg) Jörgensen, <i>Salpingella curta</i> Kofoid &amp; Campbell</p> <p>Copepods - various</p>	2.15 x 10 <sup>-9</sup> to 2.51 x 10 <sup>-8</sup>	Eppley et al. (1978)
Aeration	Glass	1.0 x 10 <sup>-3</sup>	<p>Ciliates – <i>Tetrahymena pyriformis</i> (Ehrenberg), <i>T. thermophila</i>, <i>T. pigmentosa</i></p>	None	Hellung-Larsen and Lyhne (1992)

Aeration	Unknown	Unknown	Diatoms - <i>Chaetoceros curvisetus</i> Cleve, <i>Skeletonema costatum</i>	None	Schöne (1970)
Aeration	Polyethylene	$1.67 \times 10^3$	Natural population of phytoplankton & zooplankton with salmonids added artificially. Phytoplanktonic species unspecified but main group enumerated.	Vertical eddy diffusivity coefficient = $0.06 \text{cm}^2/\text{s}$ (Steele et al., 1977).	Sonntag and Parsons (1979)
Aeration	Acrylate	$3.4 \times 10^{-3}$	Diatom – <i>Phaeodactylum tricornutum</i>	None	Thomas et al. (1984a)
Aeration	Acrylate	$3.4 \times 10^{-3}$	Green algae – <i>Dunaliella primolecta</i> Butcher & <i>Tetraselmis suecica</i> Butcher.	None	Thomas et al. (1984b)
Aeration	Acrylate	$3.4 \times 10^{-3}$	Golden algae - <i>Isochrysis</i> (Tahitian strain) & <i>Microchloropsis salina</i> (D.J.Hibbard) M.W.Fawley, I.Jameson & K.P.Fawley <sup>b</sup>	None	Thomas et al. (1984c)
Aeration	Glass	$4.0 \times 10^{-5}$	Dinoflagellate – <i>Cryptocodinium cohnii</i>	None	Tuttle and Loeblich (1975)
Convective heating	Polyethylene	$2.03 \times 10^0$	None	Dye injection homogenisation timed	Båmstedt and Larsson (2018)

Couette	Unspecified	$1.00 \times 10^{-3}$	Diatom - <i>Skeletonema</i> sp., <i>Chaetoceros</i> sp.	Converted using Equation (6) $3.42 \times 10^{-5}$	Bergkvist et al. (2018)
Couette	Unknown	Unknown	Dinoflagellate - <i>Alexandrium minutum</i> Halim	$1.64 \times 10^{-2}$ (Berdalet et al., 2007)	Chen et al. (1998)
Couette	Acrylate / steel	$4.16 \times 10^{-4}$	Green algae - <i>Chlorella</i> sp.	Converted using Equation (6) $1.28 \times 10^{-2}$	Davis et al. (1953)
Couette	Glass	$8.78 \times 10^{-4}$	Dinoflagellate – <i>Lingulodinium polyedra</i> <sup>c</sup>	Converted using Equation (6) $7.96 \times 10^{-9}$ to $1.82 \times 10^{-3}$	Gibson and Thomas (1995)
Couette	Unspecified	$8.79 \times 10^{-4}$	Green algae – <i>Desmodesmus communis</i> (E.Hegewald) E.Hegewald <sup>k</sup>	$1.27 \times 10^{-3}$ to $3.13 \times 10^{-1}$	Hondzo et al. (1997)
Couette	Glass	$1.56 \times 10^{-4}$	Dinoflagellate – <i>Lingulodinium polyedra</i> <sup>c</sup>	$1.00 \times 10^{-5}$ to $3.50 \times 10^{-4}$	Juhl and Latz (2002)
Couette	Glass	$1.56 \times 10^{-4}$	Dinoflagellate – <i>Lingulodinium polyedra</i> <sup>c</sup>	Converted using Equation (6) $1.88 \times 10^{-5}$	Juhl et al. (2000)
Couette	Acrylate	$3.91 \times 10^{-4}$	Dinoflagellate – <i>Alexandrium catenella</i> (Whedon & Kofoid) Balech <sup>d</sup>	$1.0 \times 10^{-5}$	Juhl et al. (2001)

Couette	Acrylate	$8.0 \times 10^{-4}$	Diatoms - <i>Skeletonema costatum</i> , <i>Thalassiosira nordenskiöldii</i> P.T. Cleve	$2.5 \times 10^{-7}$	Karp-Boss and Jumars (1998)
Couette	Acrylate	$8.0 \times 10^{-4}$	Dinoflagellates - <i>Glenodinium foliaceum</i> F.Stein, <i>Alexandrium catenella</i> <sup>d</sup>	$1.0 \times 10^{-8}$ to $1.0 \times 10^{-5}$	Karp-Boss et al. (2000)
Couette	Acrylate	$2.38 \times 10^{-4}$	Dinoflagellates – <i>Lingulodinium polyedra</i> <sup>c</sup> , <i>Pyrocystis noctiluca</i> Murray ex Haeckel, <i>P. fusiformis</i>	Converted using Equation (6) Large tanks = $9.65 \times 10^{-4}$ to $6.86 \times 10^{-1}$ Small tanks = $3.86 \times 10^{-3}$ to $2.75 \times 10^0$	Latz et al. (1994)
Couette	Unspecified	$1.23 \times 10^{-3}$	Cyanobacteria – <i>Nodularia sphaerocarpa</i> Bornet & Flahault, <i>N. spumigena</i> Mertens ex Bornet & Flahault	$4.66 \times 10^{-6}$ to $3.23 \times 10^{-4}$	Moisander et al. (2002)
Couette	Acrylate	$6.45 \times 10^{-4}$	Diatom – <i>Ditylum brightwellii</i> (T.West) Grunow	$5.94 \times 10^{-11}$ to $5.0 \times 10^{-8}$	Pasciak and Gavis (1975)
Couette	Polycarbonate	$1.51 \times 10^{-4}$	Dinoflagellate – <i>Pfiesteria piscicida</i> Steidinger & J.M.Burkholder with cryptophyte food source <i>Storeatula major</i> D.R.A.Hill	$2.38 \times 10^{-10}$ to $2.88 \times 10^{-8}$	Stoecker et al. (2006)



Couette	Glass	$6.45 \times 10^{-4}$	Dinoflagellate – <i>Lingulodinium polyedra</i> <sup>c</sup>	$4.50 \times 10^{-6}$ to $1.64 \times 10^{-2}$	Thomas and Gibson (1990a)
Couette	Glass	$6.45 \times 10^{-4}$	Dinoflagellate – <i>Lingulodinium polyedra</i> <sup>c</sup>	$1.80 \times 10^{-5}$ to $1.64 \times 10^{-2}$	Thomas and Gibson (1990b)
Couette	Glass	Unspecified	Dinoflagellate – <i>Akashiwo sanguinea</i> <sup>e</sup>	$2.8 \times 10^{-7}$ to $1.8 \times 10^{-3}$	Thomas and Gibson (1992)
Couette	Unknown	Unknown	Dinoflagellates – <i>Akashiwo sanguinea</i> <sup>e</sup> , <i>Prorocentrum micans</i> Ehrenberg	$4.6 \times 10^{-4}$ (Berdalet et al., 2007)	Tynan (1993)
Dialysis chamber	Glass	$6.5 \times 10^{-4}$	Natural population including: Diatom – <i>Scenedesmus</i> sp., <i>Cymbella</i> sp. <i>Navicula</i> sp., <i>Diatoma</i> sp. Green Algae – <i>Chlamydomonas</i> sp. Cryptophyte – <i>Cryptomonas</i> sp.	None	Köhler (1997)

Grid - horizontal	Glass	$4.9 \times 10^{-3}$	Green Algae – <i>Nephroselmis olivacea</i> F.Stein, <i>Cryptomonas curvata</i> Ehrenberg, <i>Spondylosium pulchellum</i> (W.Archer) W.Archer, <i>Pediastrum boryanum</i> (Turpin) Meneghini  Diatoms – <i>Asterionella formosa</i> Hassall, <i>Aulacoseira granulata</i> (Ehrenberg) Simonsen	$7.9 \times 10^{-5}$ to $7.8 \times 10^{-3}$	Fraisse et al. (2015)
Grid - horizontal	Acrylate	$9.28 \times 10^{-4}$	Dinoflagellate – <i>Heterosigma akashiwo</i> (Y.Hada) Y.Hada ex Y.Hara & M.Chihara	$2.0 \times 10^{-9}$ to $1.6 \times 10^{-8}$	Linares (2015)
Grid - horizontal	Unspecified	$6.65 \times 10^{-3}$	Dinoflagellate – <i>Phaeocystis globosa</i>	$1.0 \times 10^{-6}$ to $1.0 \times 10^{-4}$	Schapira et al. (2006)
Grid - horizontal	Acrylate	$3.05 \times 10^{-2}$	Green algae – <i>Selenastrum capricornutum</i>	$9.60 \times 10^{-9}$ to $1.25 \times 10^{-6}$	Warnaars et al. (2006)
Grid - vertical	Acrylate	$3.0 \times 10^{-2}$	Natural population with a focus on phytoplankton biomass and copepod <i>Acartia italica</i> Steuer	Vertical eddy diffusivity = $0.5 \text{ cm}^2/\text{s}$ (unstirred) / $1 \text{ to } 5 \text{ cm}^2/\text{s}$ (stirred).	Alcaraz et al. (1988)
Grid - vertical	Acrylate	$2.92 \times 10^{-1}$	Marine snow – Diatom aggregates of <i>Chaetoceros</i> sp. and <i>Nitzschia</i> sp.	$1.0 \times 10^{-7}$ to $1.0 \times 10^{-4}$	Allredge et al. (1990)

Grid - vertical	Acrylate	$1.5 \times 10^{-2}$	Natural population (filtered through a 150 $\mu\text{m}$ mesh) including: Bacteria – <i>Synechococcus</i> sp., <i>Prochlorococcus</i> sp.	$5.5 \times 10^{-6}$	Arin et al. (2002);
Grid - vertical	Acrylate	$1.5 \times 10^{-2}$	Natural population (filtered through a 150 $\mu\text{m}$ mesh) including: Diatoms – <i>Chaetoceros</i> sp, <i>Pseudo-nitzschia</i> sp	$5.5 \times 10^{-6}$	Maar et al. (2002)
Grid - vertical	Acrylate	$2.60 \times 10^0$	Natural population (filtered through 250 $\mu\text{m}$ filter) including: Diatoms - <i>Chaetoceros</i> sp., <i>Cylindrotheca closterium</i> (Ehrenberg) Reimann & J.C.Lewin, <i>Dactyliosolen fragilissimus</i> (Bergon) Hasle, <i>Nitzschia longissima</i> (Brébisson) Ralfs, <i>Skeletonema costatum</i> , <i>Thalassiosira</i> sp.	$2.0 \times 10^{-9}$ to $1.0 \times 10^{-4}$	Beauvais et al. (2006)
Grid - vertical	Glass	$1.0 \times 10^{-3}$	Dinoflagellates – <i>Akashiwo sanguinea</i> <sup>e</sup>	$2.0 \times 10^{-3}$	Berdalet (1992)
Grid - vertical	Glass	$4.0 \times 10^{-3}$	Dinoflagellates - <i>Alexandrium minutum</i> , <i>Akashiwo sanguinea</i> <sup>e</sup>	$1 \times 10^{-4}$	Berdalet and Estrada (1993)

Grid- vertical	Acrylate	1.38 x 10 <sup>-2</sup>	Bacteria – <i>Vibrio splendidus</i> Flagellate – <i>Paraphysomonas</i> sp.	1.00 x 10 <sup>-5</sup> to 1.35 x 10 <sup>-5</sup>	Delaney (2003)
Grid - vertical	Acrylate	2.0 x 10 <sup>-3</sup>	Ciliate – <i>Strombidium sulcatum</i> Claparède & Lachmann	5.0 x 10 <sup>-7</sup> to 2.0 x 10 <sup>-4</sup>	Dolan et al. (2003)
Grid - vertical	Acrylate	3.0 x 10 <sup>-2</sup>	Natural population including:  Diatoms – <i>Chaetoceros</i> sp., <i>Thalassiosira</i> sp., <i>Leptocylindrus danicus</i> Cleve, <i>Skeletonema</i> <i>costatum</i> , <i>Cylindrotheca closterium</i>  Dinoflagellates – <i>Protoperidinium</i> sp, <i>Scrippsiella trochoidea</i> (F.Stein) A.R.Loeblich  III  Haptophyte – <i>Emiliana huxleyi</i> (Lohmann)  W.W.Hay & H.P.Mohler	Vertical eddy diffusivity = 0.5 cm <sup>2</sup> /s (unstirred) / 1 to 5 cm <sup>2</sup> /s (stirred).	Estrada et al. (1987)

Grid - vertical	Polyethylene	$2.50 \times 10^0$	Natural population filtered through 250µm filter including: <i>Chaetoceros</i> sp., <i>Cylindrotheca closterium</i> , <i>Dactyliosolen fragilissimus</i> , <i>Nitzschia longissima</i> , <i>Skeletonema costatum</i> , <i>Thalassiosira</i> sp. (Beauvais et al., 2006)	$1.0 \times 10^{-7}$ to $1.0 \times 10^{-6}$	(Guadayol et al., 2009a)
Grid - vertical	Acrylate	$2.0 \times 10^{-3}$	Dinoflagellate – <i>Oxyrrhis marina</i> Dujardin Haptophyte – <i>Isochrysis</i> sp.	$1.0 \times 10^{-8}$ to $1.0 \times 10^{-4}$	Havskum (2003)
Grid - vertical	Acrylate	$2.0 \times 10^{-3}$	Dinoflagellate – <i>Kryptoperidinium triquetrum</i> (Ehrenberg) U.Tillmann, M. Gottschling, M.Elbrächter, W.-H.Kusber & M.Hoppenrath <sup>f</sup>	$1.0 \times 10^{-8}$ to $1.0 \times 10^{-4}$	Havskum and Hansen (2006)
Grid - vertical	Acrylate	$2.0 \times 10^{-3}$	Dinoflagellates – <i>Fragilidium subglobosum</i> & <i>Tripos muelleri</i> Bory <sup>g</sup>	$1.0 \times 10^{-8}$ to $1.0 \times 10^{-4}$	Havskum et al. (2005)
Grid - vertical	Fibreglass	3.02E+00	Natural population (phytoplankton dominated by <i>Anabaena</i> sp.)	$2.0 \times 10^{-4}$ to $3.80 \times 10^{-3}$	Howarth et al. (1993)
Grid - vertical	Acrylate	$2.60 \times 10^0$	see Beauvais et al. (2006)	$2.0 \times 10^{-9}$ to $1.0 \times 10^{-4}$	Iversen et al. (2009)

Grid - vertical	Unspecified	Unspecified	Dinoflagellates – <i>Peridiniella danica</i> (Paulsen) Y.B.Okolodkov & J.D.Dodge, <i>Gyrodinium dominans</i> Hulbert, <i>Oxyrrhis marina</i> Ciliate – <i>Mesodinium pulex</i> Claparède & Lachmann	1.2 x 10 <sup>-6</sup>	Martínez et al. (2017)
Grid - vertical	Unspecified	2.40 x 10 <sup>0</sup>	Natural population filtered through 250µm filter – no specific species reported.	1.0 x 10 <sup>-7</sup> to 1.0 x 10 <sup>-4</sup>	Metcalfe et al. (2004)
Grid - vertical	Polyethylene	2.70 x 10 <sup>1</sup>	Natural plankton population including: Flagellate – <i>Ebria tripartita</i> (Schumann) Lemmermann Diatom – <i>Skeletonema costatum</i> Ciliate – <i>Mesodinium rubrum</i> (Lohmann) Leegard, <i>Cyclotrichium</i> sp. Copepods – <i>Calanus helgolandicus</i> Claus, <i>Calanus finmarchicus</i> Gunnerus	5.3 x 10 <sup>-9</sup> to 1.7 x 10 <sup>-7</sup> (Svensen et al., 2001)	Nejstgaard et al. (2001a)

Grid - vertical	Polyethylene	2.70 x 10 <sup>1</sup>	<p>Natural plankton population including:</p> <p>Flagellate – <i>Octactis speculum</i> (Ehrenberg)</p> <p>F.H.Chang, J.M.Grieve &amp; J.E.Sutherland <sup>1</sup>,</p> <p><i>Emiliana huxleyi</i>, <i>Ebria tripartita</i></p> <p>Diatom – <i>Skeletonema costatum</i>, <i>Amphiprora sp</i></p> <p>Ciliates – <i>Strombidium spp.</i> and <i>Strombilidium spp.</i></p> <p>Copepods – <i>Calanus helgolandicus</i></p>	<p>5.3 x 10<sup>-9</sup> to 1.7 x 10<sup>-7</sup></p> <p>(Nerheim et al., 2002)</p>	<p>Nejstgaard et al. (2001b)</p>
-----------------	--------------	------------------------	---	---	----------------------------------

Grid - vertical	Unspecified	$1.30 \times 10^1$	<p>Natural population including:</p> <p>Dinoflagellates – <i>Peridinium</i> sp.</p> <p>Diatoms – <i>Skeletonema costatum</i>, <i>Chaetoceros compressus</i> Lauder, <i>Chaetoceros affinis</i> Lauder, <i>Chaetoceros didymus</i> Ehrenberg, <i>Chaetoceros perpusillus</i> Cleve, <i>Cylindrotheca fusiformis</i> Reimann &amp; J.C.Lewin, <i>Leptocylindricus danicus</i> Cleve, <i>Rhizosolenia delicatula</i> Cleve</p> <p>Golden Algae – <i>Dinobyron</i> sp.</p> <p>Copepods - various</p>	None	Oviatt (1981)
Grid - vertical	Glass	$1.0 \times 10^{-4}$	<p>Flagellate – <i>Paraphysomonas imperforata</i></p> <p>I.A.N.Lucas</p>	$8.5 \times 10^{-5}$ to $8.6 \times 10^{-1}$	Peters and Gross (1994)
Grid - vertical	Glass	$1.0 \times 10^{-4}$	<p>Flagellate – <i>Paraphysomonas imperforata</i></p>	$5.0 \times 10^{-6}$ to $1.5 \times 10^{-3}$	Peters et al. (1996)
Grid - vertical	Acrylate	$1.5 \times 10^{-2}$	<p>Natural population – no species identified but groups of bacteria, flagellates and ciliates.</p>	$5.3 \times 10^{-6}$ to $5.9 \times 10^{-6}$	Peters et al. (2002)



Grid - vertical	Acrylate	$1.7 \times 10^{-2}$	Cyanobacteria – <i>Microcystis aeruginosa</i> (Kützing) Kützing	Turbulent intensity ranged from $7.1 \times 10^{-3}$ and $7.04 \times 10^{-2}$ m/s	Regel et al. (2004)
Grid - vertical	Glass	$2.5 \times 10^{-2}$	Diatom – <i>Phaeodactylum tricornutum</i> . Dinoflagellate – <i>Brachionomonas submarina</i> Bohlin	$2.3 \times 10^{-4}$ to $2.3 \times 10^{-1}$	Savidge (1981)
Grid - vertical	Polycarbonate	$1.2 \times 10^{-2}$	Dinoflagellates – <i>Alexandrium catenella</i> <sup>d</sup> , <i>A. tamarense</i> <sup>h</sup> , <i>Tripos fusus</i> (Ehrenberg) F.Gómez <sup>j</sup> , <i>Tripos muelleri</i> <sup>g</sup> , <i>Gymnodinium catenatum</i> H.W.Graham, <i>Gyrodinium sp.</i> , <i>Lingulodinium polyedra</i> <sup>c</sup> , <i>Pyrocystis fusiformis</i> , <i>P. noctiluca</i>	$1.0 \times 10^{-8}$ to $1.0 \times 10^{-4}$	Sullivan and Swift (2003)

Grid - vertical	Polyethylene	$2.70 \times 10^1$	Diatoms – <i>Chaetoceros socialis</i> Flagellates – <i>Resultor micron</i> (Thronsen) Moestrup, <i>Nephroselmis minuta</i> (N.Carter) Butcher Haptophytes – <i>Phaeocystis pouchetii</i> (Hariot) Lagerheim Dinoflagellates - unspecified	$5.3 \times 10^{-9}$ to $1.9 \times 10^{-7}$	Svensen et al. (2001)
Inversion	Acrylate	$7.68 \times 10^{-8}$	Raphidophyte – <i>Heterosigma akashiwo</i> (primarily)	$3.0 \times 10^{-8}$	Sengupta et al. (2017)
Magnetic	Glass	$1.0 \times 10^{-4}$	Dinoflagellates – <i>Scrippsiella lachrymosa</i> J.Lewis ex Head	None	Smith and Persson (2005)
Magnetic	Glass	$4.0 \times 10^{-5}$	Dinoflagellate – <i>Cryptocodinium cohnii</i>	None	Tuttle and Loeblich (1975)
Paddles	Unspecified	Unspecified	Dinoflagellate – <i>Kryptoperidinium triquetrum</i> <sup>f</sup> , <i>Alexandrium tamarense</i> <sup>h</sup> Diatom – <i>Skeletonema costatum</i>	$1.0 \times 10^{-5}$	Dempsey (1982)

Paddles	PVC	1.30 x 10 <sup>1</sup>	Natural population including: Diatom – <i>Skeletonema costatum</i> Zooplankton – various copepods	None	Donaghay and Klos (1985)
Paddles	Glass	3.78 x 10 <sup>-2</sup>	Diatom – <i>Thalassiosira weissflogii</i> (Grunow) G.A.Fryxell and Hasle, <i>Skeletonema costatum</i> Cryptomonad – <i>Rhodomonas salina</i> (Wislouch) D.R.A.Hill & R.Wetherbee Chlorophyte – <i>Dunaliella tertiolecta</i> Butcher	1.1 x 10 <sup>-4</sup> to 4.0 x 10 <sup>-4</sup>	Garrison and Tang (2014)
Paddles	Acrylate	1.3 x 10 <sup>-1</sup>	Natural population including: Cyanobacteria - <i>Oscillatoria</i> spp, <i>Prochlorothrix hollandica</i> Burger-Wiersma, Stal & Mur	None	Kromkamp et al. (1992)
Paddles	Fibreglass	1.00E+00	Natural population – no species identified but chlorophyll-a and other pigments used to quantify populations of diatoms, cyanobacteria and cryptophytes.	3.00 x 10 <sup>-7</sup> to 6.89 x 10 <sup>-5</sup>	Petersen et al. (1998)
Paddles	Natural	Unspecified	Cyanobacteria – <i>Arthrospira</i> sp. (aka <i>Spirulina</i> )	None	Richmond and Vonshak (1978)

Paddles	Acrylate	$1.3 \times 10^{-1}$	Cyanobacteria – <i>Prochlorothrix hollandica</i>	None	Rijkeboer et al. (1990)
Paddles	Unknown	Unknown	Diatoms - <i>Asterionellopsis glacialis</i> (Castracane) Round, <i>Skeletonema costatum</i>	Unknown	Thomas et al. (1997)
Pumping	Acrylate	$7.5 \times 10^{-2}$	Dinoflagellates - <i>Lingulodinium polyedra</i> <sup>c</sup>	Shear stress ranged from 0.2 N/m <sup>2</sup> to 10 N/m <sup>2</sup>	Latz and Rohr (1999)
Pumping	Acrylate	$7.5 \times 10^{-2}$	Dinoflagellates – <i>Tripos fusus</i> <sup>j</sup> , <i>Ceratocorys horrida</i> , <i>Lingulodinium polyedra</i> <sup>c</sup> , <i>Pyrocystis fusiformis</i>	Shear stress ranged from 0.2 N/m <sup>2</sup> to 10 N/m <sup>2</sup>	Latz et al. (2004)
Pumping	Fibreglass	$4.15 \times 10^0$	Diatom – <i>Phaeodactylum tricornutum</i>	Shear stress ranged from 0.02 N/m <sup>2</sup> to 0.3 N/m <sup>2</sup>	Laws et al. (1983)
Pumping	Acrylate	$5.0 \times 10^{-2}$	Natural plankton population including: Cyanobacteria - <i>Limnothrix</i> sp., <i>Aphanizomenon</i> sp. Yellow-green algae - <i>Tribonema</i> sp. Green algae - <i>Closterium</i> sp., <i>Monoraphidium</i> sp.	Flow of 2.5 mL/s resulting in a mean upward velocity of $7.6 \pm$ 1.4 mm/s.	Pannard et al. (2007)

Pumping	Steel	$7.5 \times 10^{-2}$	Dinoflagellates – <i>Lingulodinium polyedra</i> <sup>c</sup> , <i>Tripos fusus</i> <sup>j</sup> , and <i>Protoperidinium</i> sp.	$5.3 \times 10^{-9}$ to $1.7 \times 10^{-7}$	Rohr et al. (1990)
Pumping	Steel	$7.5 \times 10^{-2}$	Dinoflagellates – <i>Lingulodinium polyedra</i> <sup>c</sup> , <i>Tripos fusus</i> <sup>j</sup> , and <i>Protoperidinium</i> sp.	$5.3 \times 10^{-9}$ to $1.7 \times 10^{-7}$	Rohr et al. (1997)
Pumping	Steel	$4.5 \times 10^{-1}$	Dinoflagellates – <i>Lingulodinium polyedra</i> <sup>c</sup> , <i>Tripos fusus</i> <sup>j</sup> , and <i>Protoperidinium</i> sp.	Mean shear stress = 11 to 13.5 dyn/cm <sup>2</sup>	Rohr et al. (2002)
Shaker - unspecified	Glass	$2.5 \times 10^{-3}$	Diatom – <i>Chaetoceras affinis</i>	None	Talling (1960)
Shaker - orbital	Glass	$3.0 \times 10^{-3}$	Dinoflagellates – <i>Akashiwo sanguinea</i> <sup>e</sup>	$2.0 \times 10^{-3}$	Berdalet (1992)
Shaker - orbital	Glass	$4.0 \times 10^{-3}$	Dinoflagellates - <i>Scrippsiella trochoidea</i> , <i>Prorocentrum micans</i>	$2.0 \times 10^{-4}$	Berdalet and Estrada (1993)
Shaker - orbital	Glass	$3.0 \times 10^{-3}$	Dinoflagellates – <i>Gymnodinium</i> sp., <i>Alexandrium minutum</i> , <i>Prorocentrum triestinum</i> J.Schiller	$2.7 \times 10^{-5}$ to $2.4 \times 10^{-3}$	Berdalet et al. (2007)
Shaker - orbital	Glass	$1.0 \times 10^{-4}$	Cyanobacteria – <i>Anabaena cylindrica</i>	None	Fogg and Than- Tun (1960)

Shaker - orbital	Glass / polycarbonate	$3.00 \times 10^{-3}$	None	$1 \times 10^{-10}$ to $1 \times 10^{-2}$	Guadayol et al. (2009b)
Shaker - orbital	Glass	$2.5 \times 10^{-5}$	Ciliates – <i>Tetrahymena pyriformis</i> , <i>T. thermophile</i> , <i>T. pigmentosa</i>	$1.17 \times 10^{-2}$ to $2.16 \times 10^{-2}$	Hellung-Larsen and Lyhne (1992)
Shaker - orbital	Glass	$3 \times 10^{-3}$	Dinoflagellates - <i>Prorocentrum micans</i> , <i>Scrippsiella trochoidea</i> , <i>Alexandrium minutum</i>	$2.7 \times 10^{-3}$	Llaveria et al. (2010)
Shaker - orbital	Glass	$1.0 \times 10^{-4}$	Diatom – <i>Ditylum brightwellii</i>	None	Pasciak and Gavis (1975)
Shaker - orbital	Polycarbonate	$2.5 \times 10^{-3}$	Diatoms – <i>Thalassiosira pseudonana</i> Hasle & Heimdal, <i>Coscinodiscus</i> sp	$1.0 \times 10^{-3}$	Peters et al. (2006)
Shaker - orbital	Unspecified	Unspecified	Dinoflagellates – <i>Peridinium cinctum</i> (O.F.Müller) Ehrenberg	$4.3 \times 10^{-3}$	Pollinger and Zemel (1981)
Shaker - orbital	Glass	$2.5 \times 10^{-4}$	Dinoflagellate – <i>Lingulodinium polyedra</i> <sup>c</sup>	$2.0 \times 10^{-2}$	Thomas and Gibson (1990b)
Shaker - orbital	Glass	$4.0 \times 10^{-5}$	Dinoflagellate – <i>Cryptocodinium cohnii</i>	None	Tuttle and Loeblich (1975)

Shaker - orbital	Glass	$5.0 \times 10^{-5}$	Dinoflagellates – <i>Alexandrium tamarense</i> <sup>h</sup>	$4.30 \times 10^{-3}$ to $1.19 \times 10^{-2}$	White (1976)
Shaker - orbital	Glass	$6.0 \times 10^{-5}$	Dinoflagellates – <i>Cryptocodinium cohnii</i> ; <i>Kryptoperidinium triquetrum</i> <sup>f</sup>	$1.0 \times 10^{-5}$ to $9.9 \times 10^{-5}$	Yeung and Wong (2003)
Shaker - orbital	Glass	$6.0 \times 10^{-5}$	Dinoflagellates – <i>Cryptocodinium cohnii</i> ; <i>Kryptoperidinium triquetrum</i> <sup>f</sup>	$1.0 \times 10^{-5}$ to $9.9 \times 10^{-5}$	Yeung et al. (2006)
Shaker - orbital	Glass	$1.25 \times 10^{-4}$	Dinoflagellates - <i>Ceratocorys horrida</i>	$1 \times 10^{-5}$ to $1 \times 10^{-4}$ (Berdalet et al., 2007)	Zirbel et al. (2000)
Shaker - reciprocal	Glass	$2.5 \times 10^{-5}$	Ciliates – <i>Tetrahymena pyriformis</i> , <i>T. thermophile</i> , <i>T. pigmentosa</i>	$1.17 \times 10^{-2}$ to $2.16 \times 10^{-2}$	Hellung-Larsen and Lyhne (1992)
Shaker - reciprocal	Glass	$2.6 \times 10^{-4}$	Dinoflagellate - <i>Lingulodinium polyedra</i> <sup>c</sup>	Estimated using Equation (2) ~10	Juhl and Latz (2002)
Wave	Unspecified	$9.90 \times 10^0$	Dinoflagellate – <i>Pyrocystis fusiformis</i>	$3.0 \times 10^{-2}$ to $3.0 \times 10^1$	Stokes et al. (2004)

- <sup>a</sup> The diatom *Pseudo-nitzschia pungens* (Grunow ex Cleve) Hasle 1993 was formerly referred to as *Nitzschia pungens* Grunow ex Cleve 1897.
- <sup>b</sup> The golden alga *Microchloropsis salina* (D.J.Hibbard) M.W.Fawley, I.Jameson & K.P.Fawley 2015 was formerly referred to as *Monallantus salina* Bourrelly 1958.
- <sup>c</sup> The dinoflagellate *Lingulodinium polyedra* (F.Stein) J.D.Dodge 2018 was formerly referred to as *L. polyedrum* Dodge 1989 & *Gonyaulax polyedra* Stein 1883.
- <sup>d</sup> The dinoflagellate *Alexandrium catenella* (Whedon & Kofoid) Balech, 1985 was formerly referred to as *Alexandrium fundyense* Balech, 1985
- <sup>e</sup> The dinoflagellate *Akashiwo sanguinea* (K. Hirasaka) Gert Hansen & Moestrup 2000 was formerly referred to as *Gymnodinium nelsonii* Martin 1929, *G. sanguineum* Hirasaka 1922 & *G. splendens* Lebour 1925.
- <sup>f</sup> The dinoflagellate *Kryptoperidinium triquetrum* (Ehrenberg) U.Tillmann, M. Gottschling, M.Elbrächter, W.-H.Kusber & M.Hoppenrath 2019 was formerly referred to as *Heterocapsa triquetra* (Ehrenberg) F.Stein 1883.
- <sup>g</sup> The dinoflagellate *Tripos muelleri* Bory 1826 was formerly referred to as *Ceratium tripos* (O.F.Müller) Nitzsch 1817.
- <sup>h</sup> The dinoflagellate *Alexandrium tamarense* (Lebour) Balech 1995 was formerly referred to as *A. tamarensis* Balech 1992, *Gonyaulax excavata* Balech 1971 & *G. tamarensis* Lebour 1925.
- <sup>i</sup> The flagellate *Octactis speculum* (Ehrenberg) F.H.Chang, J.M.Grieve & J.E.Sutherland 2017 was formerly referred to as *Dictyocha speculum* Ehrenberg 1839.
- <sup>j</sup> The dinoflagellate *Tripos fusus* (Ehrenberg) F.Gómez 2013 was formerly referred to as *Ceratium fusus* (Ehrenberg) Dujardin 1841.
- <sup>k</sup> The green alga *Desmodesmus communis* (E.Hegewald) E.Hegewald 2000 was formerly referred to as *Scenedesmus quadricauda* Chodat 1926



The presence of an 'unknown' indicates a paper that was not available; 'unspecified' indicates that this information was absent from the paper.